



UNIVERSIDAD DE INVESTIGACIÓN DE TECNOLOGÍA EXPERIMENTAL YACHAY

Escuela de Ciencias Físicas y Nanotecnología

TÍTULO: Study of the Starobinsky inflationary model into the slow-roll approximation

Trabajo de integración curricular presentado como requisito para
la obtención
del título de Físico

Autor:

Orozco Sánchez Esteban Alejandro

Tutor:

Dr. Rojas Cely Clara Inés, PhD.

Urcuquí, mayo 2021

SECRETARÍA GENERAL
(Vicerrectorado Académico/Cancillería)
ESCUELA DE CIENCIAS FÍSICAS Y NANOTECNOLOGÍA
CARRERA DE FÍSICA
ACTA DE DEFENSA No. UITEY-PHY-2021-00005-AD

A los 27 días del mes de mayo de 2021, a las 16:00 horas, de manera virtual mediante videoconferencia, y ante el Tribunal Calificador, integrado por los docentes:

Presidente Tribunal de Defensa	Dr. RAMIREZ VELASQUEZ JOSE MANUEL , Ph.D.
Miembro No Tutor	Dr. YEPES RAMIREZ, HAROLD , Ph.D.
Tutor	Dra. ROJAS CELY CLARA INES , Ph.D.

El(la) señor(ita) estudiante **OROZCO SANCHEZ, ESTEBAN ALEJANDRO**, con cédula de identidad No. **0604194134**, de la **ESCUELA DE CIENCIAS FÍSICAS Y NANOTECNOLOGÍA**, de la Carrera de **FÍSICA**, aprobada por el Consejo de Educación Superior (CES), mediante Resolución **RPC-SO-39-No.456-2014**, realiza a través de videoconferencia, la sustentación de su trabajo de titulación denominado: **Study of the Starobinsky inflationary model into the slow-roll approximation** , previa a la obtención del título de **FÍSICO/A**.

El citado trabajo de titulación, fue debidamente aprobado por el(los) docente(s):

Tutor	Dra. ROJAS CELY CLARA INES , Ph.D.
--------------	------------------------------------

Y recibió las observaciones de los otros miembros del Tribunal Calificador, las mismas que han sido incorporadas por el(la) estudiante.

Previamente cumplidos los requisitos legales y reglamentarios, el trabajo de titulación fue sustentado por el(la) estudiante y examinado por los miembros del Tribunal Calificador. Escuchada la sustentación del trabajo de titulación a través de videoconferencia, que integró la exposición de el(la) estudiante sobre el contenido de la misma y las preguntas formuladas por los miembros del Tribunal, se califica la sustentación del trabajo de titulación con las siguientes calificaciones:

Tipo	Docente	Calificación
Presidente Tribunal De Defensa	Dr. RAMIREZ VELASQUEZ JOSE MANUEL , Ph.D.	9,2
Tutor	Dra. ROJAS CELY CLARA INES , Ph.D.	9,9
Miembro Tribunal De Defensa	Dr. YEPES RAMIREZ, HAROLD , Ph.D.	8,5

Lo que da un promedio de: **9.2 (Nueve punto Dos)**, sobre 10 (diez), equivalente a: **APROBADO**

Para constancia de lo actuado, firman los miembros del Tribunal Calificador, el/la estudiante y el/la secretario ad-hoc.

Certifico que *en cumplimiento del Decreto Ejecutivo 1017 de 16 de marzo de 2020, la defensa de trabajo de titulación (o examen de grado modalidad teórico práctica) se realizó vía virtual, por lo que las firmas de los miembros del Tribunal de Defensa de Grado, constan en forma digital.*

OROZCO SANCHEZ, ESTEBAN ALEJANDRO
Estudiante

ESTEBAN ALEJANDRO OROZCO SANCHEZ
 Firmado digitalmente por ESTEBAN ALEJANDRO OROZCO SANCHEZ
 Fecha: 2021.05.28 13:18:47 -05'00'

Dr. RAMIREZ VELASQUEZ JOSE MANUEL , Ph.D.
Presidente Tribunal de Defensa

JOSE MANUEL RAMIREZ VELASQUEZ
 Digitally signed by JOSE MANUEL RAMIREZ VELASQUEZ
 Date: 2021.05.28 09:13:06 -05'00'

Dra. ROJAS CELY CLARA INES , Ph.D.
Tutor

CLARA INES ROJAS CELY
 Digitally signed by CLARA INES ROJAS CELY
 Date: 2021.05.27 17:17:56 -05'00'

Dr. YEPES RAMIREZ, HAROLD , Ph.D.
Miembro No Tutor

**HAROLD
YEPES
RAMIREZ**  Firmado
digitalmente por
HAROLD YEPES
RAMIREZ
Fecha: 2021.05.28
09:17:59 -05'00'

CIFUENTES TAFUR, EVELYN CAROLINA
Secretario Ad-hoc

EVELYN
CAROLINA
CIFUENTES
TAFUR  Digitally signed by
EVELYN CAROLINA
CIFUENTES TAFUR
Date: 2021.05.27
17:15:59 -05'00'

Autoría

Yo, **Esteban Alejandro Orozco Sánchez**, con cédula de identidad **0604194134**, declaro que las ideas, juicios, valoraciones, interpretaciones, consultas bibliográficas, definiciones y conceptualizaciones expuestas en el presente trabajo; así como, los procedimientos y herramientas utilizadas en la investigación, son de absoluta responsabilidad de el autor del trabajo de integración curricular. Así mismo, me acojo a los reglamentos internos de la Universidad de Investigación de Tecnología Experimental Yachay.

Urcuquí, Marzo del 2021.

Esteban Alejandro Orozco Sánchez
CI: 0604194134

Autorización de publicación

Yo, **Esteban Alejandro Orozco Sánchez**, con cédula de identidad **0604194134**, cedo a la Universidad de Tecnología Experimental Yachay, los derechos de publicación de la presente obra, sin que deba haber un reconocimiento económico por este concepto. Declaro además que el texto del presente trabajo de titulación no podrá ser cedido a ninguna empresa editorial para su publicación u otros fines, sin contar previamente con la autorización escrita de la Universidad.

Asimismo, autorizo a la Universidad que realice la digitalización y publicación de este trabajo de integración curricular en el repositorio virtual, de conformidad a lo dispuesto en el Art. 144 de la Ley Orgánica de Educación Superior.

Urququí, Marzo del 2021.

Esteban Alejandro Orozco Sánchez
CI: 0604194134

Acknowledgements

First, I want to express my gratitude to Clara Rojas, for her attitude and unconditional support to carry out this degree project. For trusting in my skills and knowledge, I will always be grateful to her.

I would like to extend my thanks to all the professors that belong to the School of Physics and Nanotechnology, for giving me their guidance to obtain the necessary knowledge to understand this beautiful world of physics, as well as for many times being more than professors, friends and guides in our lives.

Finally I dedicate this work to my family, Miriam, Andrés, Pedro and Dani. At the same time to my second family, my unconditional friends of Yachay and my friends from my childhood. Total thanks.

Abstract

Historically, the inflation was introduced to solve the problems of the Bing-Bang theory, i.g. flatness, horizon and multipole problem, however, it has another important characteristic, it generates a primordial spectrum of density perturbations almost scale invariant and of the form of a power-law, that causes anisotropies in the cosmic microwave background (CMB) temperature and it is the seeds for large scale structure in the universe. The anisotropies of the CMB allow us to probe the primordial power spectrum generated in an epoch of cosmological inflation. The study of several models of inflation has been object to research in the last two decades. According to the recent results reported by the satellite Planck the Starobinsky model $V = \frac{3}{4}M^2 \left(1 - e^{-\sqrt{2/3}\phi}\right)^2$ is one of the main inflationary models that best fits with observations. The present work has the main objective to use the slow-roll solutions with the CAMB program to obtain the angular power spectrum for the Starobinsky inflationary model and compare our results with those reported by the satellite Planck 2018. The recreated temperature power spectrum shows small differences in amplitude and angular scales compared with the Plank results, this differences are directly related with some changes in the physical process observed at early Universe epoch. One of the main results is the dependence of cosmic observables values with the shape of the temperature power spectrum, from the Starobinsky model is obtained an age of universe of 13.798 ± 0.007 Gyr, a matter and baryon density of $\Omega_m = 1.315 \pm 0.0015$, $\Omega_b h^2 = 0.0223 \pm 0.0004$, respectively. Also, the scalar spectral index shows a value of $n_t = 0.9653 \pm 0.0004$. Finally, we motivate the study of the most intensive peaks of the angular power spectrum, in order to observe better the dependencies of cosmic parameters with the amplitude of the peaks.

Keywords: Inflation, angular power spectrum, Starobinsky potential, cosmic parameters.

Abstract

Históricamente, la inflación se introdujo para resolver los problemas de la teoría de Bing-Bang, tales como, el problema de planitud, el problema de horizonte y el problema de monopolos magnéticos. Sin embargo, tiene otra característica importante, genera un espectro primordial de perturbaciones de densidad casi invariantes de escala, y de la forma de una ley de potencia, la cual provoca anisotropías en la temperatura de la radiación de fondo de microondas (CMB) y es la semilla para la formación de grandes estructuras en el universo. Las anisotropías del CMB nos permiten sondear el espectro de energía primordial generado en una época de inflación. El estudio de varios modelos de inflación ha sido objeto de investigación en las últimas dos décadas. Según los recientes resultados reportados por el satélite Planck, el modelo de Starobinsky $V = \frac{3}{4}M^2 \left(1 - e^{-\sqrt{2/3}\phi}\right)^2$ es uno de los principales modelos inflacionarios que mejor se ajusta con las observaciones. El presente trabajo tiene como objetivo principal utilizar las soluciones slow-roll con el programa CAMB para obtener el espectro de potencia angular para el modelo inflacionario de Starobinsky, y comparar nuestros resultados con los reportados por el satélite Planck en 2018. El espectro de potencia de temperatura recreado muestra pequeñas diferencias en amplitud y escalas angulares en comparación con los resultados de Plank, estas diferencias están directamente relacionadas con algunos cambios en los procesos físicos observados en la época del Universo temprano. Uno de los principales resultados es la dependencia en los valores de los observables cósmicos con la forma del espectro de potencia de temperatura. Del modelo de Starobinsky se obtiene una edad del universo de 13.798 ± 0.007 Gyr, una materia y densidad bariónica de $\Omega_m = 1.315 \pm 0.0015$, $\Omega_b h^2 = 0.0223 \pm 0.0004$, respectivamente. Además, el índice espectral escalar muestra un valor de $n_t = 0.9653 \pm 0.0004$. Finalmente, motivamos el estudio de los picos más intensivos del espectro de potencia angular, con el fin de observar mejor las dependencias de los parámetros cósmicos con la amplitud de los picos.

Keywords: Inflación, espectro de potencia angular, potencial de Starobinsky, parámetros cósmicos.

Contents

List of Figures	xiv
List of Tables	xv
1 Introduction	1
1.1 Problem Statement	2
1.1.1 Recreation of the temperature power spectrum	2
1.2 General and Specific Objectives	3
1.3 Outline	3
2 Methodology	5
2.1 The cosmological model and its problems	5
2.1.1 The standard Big-Bang theory	5
2.1.2 Flatness problem	7
2.1.3 Horizon problem	8
2.1.4 Monopole problem	8
2.2 Inflation	9
2.2.1 Solution to the flatness problem	9
2.2.2 Solution to the horizon problem	10
2.2.3 Solution to the monopole problem	10
2.2.4 Scalar fields in cosmology	10
2.3 Slow-roll approximation	11
2.3.1 Amount of inflation	13
2.4 Starobinsky inflationary model	13
2.4.1 Equations of motion with Starobinsky model	14
2.5 The CMB angular power spectrum	15
2.5.1 Primordial cosmic fluctuations	15
2.5.2 Temperature anisotropies	16

2.5.3	The power spectrum in terms of tensor and scalar spectral index	17
3	Results & Discussion	19
3.1	Angular power spectrum with S.model	19
3.1.1	Relative error and percentage of relative error	21
3.2	Sachs-Wolfe plateau region	23
3.3	Acoustic Peak region	24
3.4	Silk Damping region	26
3.5	Methodology of results	28
4	Conclusions & Outlook	31
	Bibliography	33

List of Figures

2.1	Starobinsky Potential	14
2.2	CMB maps at different multipole moments	17
3.1	CMB temperature power spectrum recreate from Starobinsky potential	20
3.2	Relative error from recreated CMB temperature power spectrum	21
3.3	Percentage of error from recreated CMB temperature power spectrum	22
3.4	Sachs-Wolfe plateau region obtained from Starobinsky model	23
3.5	Acoustic Peak region obtained from Starobinsky model	25
3.6	Silk Damping region obtained from Starobinsky model	27

List of Tables

3.1	Peaks of the CMB TT power spectra in the "Acoustic Peak" region recreated by the Starobinsky model and reported by Planck satellite ¹	26
3.2	Cosmic parameters obtained from the Starobinsky model compared with the cosmic parameters reported by Planck ¹	27
3.3	Values of scalar and tensor spectral indices, their corresponding running indices and tensor-to-scalar ratio, obtained from the Starobinsky model in a slow-roll approximation and reported by Planck satellite ^{1,2}	29

Chapter 1

Introduction

The origin and evolution of our Universe always has been a topic that has aroused curiosity in us, this curiosity has functioned as the main fuel for the creation and improvement of the theories around the early Universe that we know at present. Since, the prediction by Alpher and Herman³ in 1948 and the discovery in 1965 by Penzias and Wilson⁴ of the Cosmic Microwave Background Radiation (CMB), has become one of the most important observational probes of the Big-Bang theory. The CMB is a relic from the recombination epoch which occurs 370,000 years after the big bang⁵. After the discovery of the CMB, the Big-Bang model of cosmology was established and the Universe has an isotropic and homogeneous nature, i.e., the Friedmann universe.

Immediately after the discovery of the CMB, the cosmologist started to look for distortions in the isotropy in the CMB radiation, which are referred to as anisotropies. This arose from the assumption that the structure in the Universe comes from small initial fluctuations by gravitational instability⁶. The first evidence of the cosmic anisotropies was a dipole which was revealed in 1969⁷, and in the late 80s it was known that temperature fluctuations correspond to $(\Delta T/T) \lesssim 10^{-4}$, discarding a purely baryonic universe and favoring a universe in which a sufficient amount of dark matter is needed. Later, in 1989 the NASA satellite COBE⁸ was launched and successfully measured the CMB spectrum and found the CMB fluctuations on the level of 10^{-5} . This observation was the pioneer to future experiments with similar objectives, e.g., Boomerang, ACBAR and ACT. But, in 2001 the WMAP⁹ and in 2009 the Planck¹ mission was launched, showing with high precision the temperature fluctuations and the slight polarization which is generated on the last scattering surface by Thomson scattering. The temperature fluctuations are observed and analysed in the angular power spectrum, which Bond and Efstathiou¹⁰ proposed to use the multipole component as an observational quantity, which is widely used at present.

The temperature fluctuations are generated by individual physical processes in the expanding Universe. However, it is possible to separate the fluctuations of the CMB in three parts with their corresponding physics. The first process was proposed by Sachs and Wolfe¹¹ in 1967, which consists in a simple redshift of CMB photons due to the density fluctuations at the last scattering surface. This effect is mainly observed at large angular scales. The second effect

is referred as acoustic oscillations. Before recombination photons, electron and protons are coupled and can be treated as a mixed compressive fluid and the density fluctuations in this fluid are acoustic waves. Therefore, the perturbations of the mixed fluid start to oscillate once they cross the sound horizon¹². In the CMB spectrum the acoustic oscillations are only observed within angular scales corresponding to the sound horizon. The third effect was pointed out by Silk in 1968 and is present on small scales, consist in density fluctuations of photons that are damped away due to diffusion. The present work follows the same distribution in order to analyse the changes in the physical process at report a different CMB temperature power spectrum.

Some cosmic parameters and observables, i.g. $\Omega_b h^2$, Ω_m , n_t and n_s , has a direct dependence on the CMB temperature spectrum. Theoretically, the shape of the temperature power spectrum depends of the cosmological model that is used to obtain it. The present work recreates the spectrum with a the Starobinsky inflationary model into the slow-roll approximation, in order to observe how well the Starobinsky model can describe the physics of our early Universe. The analysis presented in this work shows how small changes in the temperature power spectrum are related with different values of cosmic parameters and observables, also this changes are related with small differences in physical processes at inflationary epoch. The natural units ($c = \hbar = 1$) are used in the whole work for simplify calculations.

1.1 Problem Statement

The standard Big-Bang theory became popular after the discovery of the cosmic microwave background radiation (CMB). However the theory do not match with the present standard model of particles by the monopole problem, also present other difficulties (the flatness problem, the horizon problem, and others). This problems are solved by inflation theory, in which are used different inflationary models, the most popular are based in a potential energy density $V(\phi)$ of some scalar field ϕ , e.g. the chaotic model, hilltop model, natural inflation model, etc. Some of these models are disadvantaged by recent Planck¹ data, but the models with low amount of tensor perturbations, i.e. small values of tensor-to-scalar ratio r are favored. One of the models that overcomes this constraints are the Starobinsky inflationary model, however the model has to match with the present observables, like cosmic anisotropies and cosmic parameters. For this reason, one of the main results of this thesis is the estimation of some cosmic observables, as the tensor n_t and scalar n_s spectral index, the running of both terms, the matter Ω_m and the baryon $\Omega_b h^2$ density and age of the Universe.

1.1.1 Recreation of the temperature power spectrum

The CMB shows an average temperature $T = 2.72K$ at almost every frequency. However, one of the main results of inflation theory was reveal small temperature fluctuations present in the CMB, which are a snapshot of the distribution of matter at early Universe. The temperature power spectrum characterizes the sizes of the temperature fluctuations as a function of the multipole moment and the angular scale. The most recent results reported by Planck¹ satellite, shows a very accurate measure of the temperature power spectrum. From this, the inflationary models can be judged

by how well they recreate the temperature power spectrum. For this reason in the present work, in order to test the inflationary Starobinsky model into the slow-roll approximation, the temperature power spectrum will be recreated and compared to the Planck data reported at today.

1.2 General and Specific Objectives

The overall objective of this work is reproduce the CMB temperature power spectrum with the Starobinsky inflationary model into the slow-roll approximation using the CAMB¹³ code. The accurate recreation of the temperature power spectrum with the Starobinsky model can be used to show how well the model is able describe the early Universe and validate the robustness of the model. After the recreation of the temperature power spectrum, the analysis and discussion around the three main regions of the spectra will be presented, in order to show how small differences in the amplitude and position of the spectra implies changes in the physics that governs the early evolution of our Universe. The study of the dependence of different cosmic parameters (scalar index, matter and baryon density and age of Universe) with the shape of the temperature power spectrum should be coherent with the previews literature, in order to "test" the results and the procedure that was followed in this work.

1.3 Outline

This work is split into four chapters, in which are given the details of the investigation performed and the physical/-mathematical principles behind them. The first chapter presents the history and the importance around the CMB temperature power spectrum which is the main result of this work.

The second chapter is Methodology, where is explained the theoretic context around the CMB temperature spectrum. From how the theory of big-bag present three main problems that inflation are able to solve, to the slow-roll approximation, how the Starobinsky inflationary model shows as a solid candidate to describe the physics of our early Universe and finally the emerge of the temperature anisotropies from the quantum fluctuations and how the power spectrum is a main tool to describe the CMB anisotropies.

The third one, Results & Discussion will address the recreated CMB temperature power spectrum with the Starobinsky inflationary model into the slow-roll approximation, Also the analysis of the respective main regions that compose the spectrum.

And finally, in the Conclusions and Outlook chapter the results and discussion around the temperature power spectrum obtained, will be summarized, also a quick view to future research in this topic is presented.

Chapter 2

Methodology

2.1 The cosmological model and its problems

2.1.1 The standard Big-Bang theory

The standard Big-Bang theory is based in the premise of modern cosmology, that tell us that the Universe is isotropic and homogeneous at large scale¹⁴. This premise are encoded in the Friedman-Robertson-Walker (FRW) metric

$$ds^2 = -dt^2 + a^2(t) \left[\frac{dr^2}{1 - kr^2} + r^2(d\theta + \sin^2 \theta d\phi^2) \right], \quad (2.1)$$

where $a(t)$ is the scale factor that describes the relative expansion of the Universe¹⁵; normalized $a(t_0) = 1$ at the present moment¹⁶. The spatial curvature is described by the constant k and can take three values, $k = 1$ for positive spatial curvature universe, $k = 0$ for spatially flat universe and $k = -1$ for negative spatial curvature universe¹⁶. The spatial variables (t, r, θ, ϕ) are in polar coordinates.

The properties of the Universe depends of the material within it, for this case the source is consider as a perfect fluid with pressure $p(t)$ and energy density $\rho(t)$ ¹⁵. The equation of state with the form $p = p(\rho)$ relate both quantities and the most popular cases are¹⁵

$$\begin{aligned} p &= \frac{\rho}{3}, & \text{radiation,} \\ p &= 0, & \text{matter,} \\ p &= -\rho, & \text{cosmological constant } \Lambda. \end{aligned} \quad (2.2)$$

The dynamics of the evolution of the Universe are described by the Einstein equations in general relativity¹⁷. The Einstein tensor relates the local space-time curvature with the local energy¹⁸, and is defined as

$$G_{\mu\nu} = R_{\mu\nu} - \frac{1}{2}g_{\mu\nu}R = 8\pi GT_{\mu\nu} - \Lambda g_{\mu\nu}, \quad (2.3)$$

where $R_{\mu\nu}$, R , $T_{\mu\nu}$, G , Λ are the Ricci tensor, Ricci scalar, energy momentum tensor, gravitational constant and cosmological constant respectively. The gravitational constant G are related with the mass of Planck M_{pl} , the speed of light c and the Planck's constant \hbar , by the relation¹⁷ $M_{pl} = (\hbar c^5/G)^{1/2}$. Remember, that natural units ($c = \hbar = 1$) are used for simplify the calculations.

For solving the Einstein equations for the FRW metric 2.1, the Ricci scalar has the form

$$R = \frac{6[k + \dot{a}^2(t) + a(t)\ddot{a}(t)]}{a^2(t)}, \quad (2.4)$$

and

$$g_{\mu\nu} = \begin{pmatrix} -1 & 0 & 0 & 0 \\ 0 & \frac{a^2(t)}{1-kr^2} & 0 & 0 \\ 0 & 0 & a^2(t)r^2 & 0 \\ 0 & 0 & 0 & a^2(t)r^2 \sin^2 \theta \end{pmatrix}. \quad (2.5)$$

The energy momentum tensor for a perfect fluid is defined as

$$T_{\mu\nu} = (\rho + P)U_\mu U_\nu + P g_{\mu\nu}, \quad (2.6)$$

where U is the 4-velocity vector field of the fluid¹⁹.

Equations of state

Running the sub-indices μ and ν and replacing (2.4), (2.6) and (2.5) in (2.3), give us the **Friedmann equation**

$$H^2 = \left(\frac{\dot{a}}{a}\right)^2 = \frac{8\pi}{3M_{pl}^2}\rho - \frac{k}{a^2}, \quad (2.7)$$

the **acceleration equation**

$$\frac{\ddot{a}}{a} = -\frac{4\pi}{3M_{pl}^2}(\rho + 3p), \quad (2.8)$$

and the **the fluid equation**¹⁵

$$\dot{\rho} + 3H(\rho + p) = 0, \quad (2.9)$$

where H is the Hubble parameter. The value of H at the present moment is known as the "Hubble constant"¹⁶, according to the measurement of Hubble telescope²⁰ has a value of

$$H_0 = H(t_0) = \left(\frac{\dot{a}}{a}\right)_{t=t_0} = 70.0_{-8.0}^{12.0} \text{ km s}^{-1} \text{ Mpc}^{-1}. \quad (2.10)$$

The Friedmann equation (2.7) can be written in terms of the density parameter Ω

$$\Omega - 1 = \frac{k}{a^2 H^2}, \quad (2.11)$$

where

$$\Omega = \frac{\rho}{\rho_c}. \quad (2.12)$$

The critical density ρ_c is defined for a given value of the Hubble parameter¹⁶ H , as

$$\rho_c = \frac{3H^2 M^2}{8\pi}, \quad (2.13)$$

and from the relation (2.12) is observed that for spatially flat Universe $k = 0$, the critical density should be the same that the energy density ($\rho = \rho_p$). For the same case ($k = 0$), the Friedman equation (2.7) takes the form

$$H^2 = \frac{3\pi}{3M_{pl}^2} \rho, \quad (2.14)$$

and (2.12), comes to

$$\Omega = 1. \quad (2.15)$$

The solution for the fluid equation (2.9) has the form

$$\rho \propto a^{-3(1+p)}, \quad (2.16)$$

replacing the three cases of (2.17) in this solution (2.16), is obtained

$$\begin{aligned} \rho &\propto a^{-4}, & \text{radiation,} \\ \rho &\propto a^{-3}, & \text{matter,} \\ \rho &\propto a^0, & \text{cosmological constant } \Lambda. \end{aligned} \quad (2.17)$$

The equations of states (2.7), (2.8) and (2.9), are the three key equations with describes how the Universe expands¹⁶.

2.1.2 Flatness problem

The flatness problem is often consider as the most impressive issue in the standard cosmology model²¹. As we saw in the last section, the spatial curvature of the universe is related with the density parameter Ω by equation (2.11)¹⁶. The case $\Omega = 1$ is an unstable equilibrium point, meaning that small deviations from this value would have significant effects on the curvature of the universe¹⁵. If the early universe was flat this value should be the same or very close to 1¹⁷. The problem is that in the standard big-bag theory the $a^2 H^2$ term of (2.11) decreases at time of radiation or matter domination epoch, this indicates that Ω tends to move way from unity with the expansion of universe¹⁷. Then, the relation between Ω and time t are

$$|\Omega - 1| \propto t, \quad \text{during radiation domination,} \quad (2.18)$$

and

$$|\Omega - 1| \propto t^{2/3}, \quad \text{during dust domination.}^{15} \quad (2.19)$$

Thus, for obtain the correct spatial-geometry is required the value of:

- $|\Omega - 1| = |\Omega_0 - 1|t/t_0$ at the present ($t_0 \approx 13.787$ Gyrs).
- $|\Omega - 1| \leq 10^{-3}$ at decoupling epoch ($t \approx 10^{13}$ sec).
- $|\Omega - 1| \leq 10^{-16}$ at nucleosynthesis epoch ($t \approx 1$ sec).
- $|\Omega - 1| \leq 10^{-64}$ at the Planck epoch ($t \approx 10^{-43}$ sec).¹⁵

There is no reason to prefer a Universe with critical density, hence $|\Omega - 1|$ should not necessary be exactly zero¹⁵. From this, at early times the value of $|\Omega - 1|$ is not fine-tuned extremely close to zero to reach the actual value observed¹⁵.

2.1.3 Horizon problem

The horizon problem is related with the premise of the large scale homogeneity²². The photons that we observe in the Cosmic Microwave Background (CMB) were emitted at the time of decoupling¹⁷. This process occurred in a spherical surfaces named the "surface of last scattering"¹⁵. The current proper distance to the last scattering surface is

$$d_p(t_0) = c \int_{t_s}^{t_0} \frac{dt}{a(t)}. \quad (2.20)$$

From the above equation is observed that the current proper distances to the last scattering surface is slightly smaller than the current horizon distance, since the scattering of the CMB photons occurred a long time ago ($t_s \ll t_0$)¹⁶. From this is observed that two points separated by 180° on the last scattering surface are so far from each other that they are causally disconnected¹⁶, meaning that they not had time to share properties, e.g. temperature. The essential problem is that at observe the CMB the photons distributed on the whole sky have nearly the same temperature $T_0 \approx 2.7255$ K at the present¹⁵. Therefore, the Big Bang model is not able to explain how the temperature of opposite directions of the sky are approximately the same¹⁵.

2.1.4 Monopole problem

The Grand Unified Theories (GUT) in particle physics refers to the theories that attempt to unify the three forces of the Standard Model (SM), i.e. strong force, weak force and electromagnetic force¹⁵. These theories describes a symmetry phase at high temperatures ($t \approx 10^{32}$ K) in the early stages of the Universe¹⁵. The decrease of the temperature causes different phase transitions that break the symmetry of the early stages¹⁵, this beak of symmetry leads to the production of "unwanted relics" as monopoles, cosmic strings, and topological defects²³. If monopoles exist is expected that behave as a matter component and are diluted slower than radiation, meaning that they would dominate the present universe²⁴. The main problem is that the existence of this monopoles violates the current observations, since the scientist have not yet discovered any magnetic monopole²⁴.

2.2 Inflation

The most simple definition of inflation is any epoch during which the scale factor of the Universe is accelerating¹⁴, i.e.,

$$\ddot{a} > 0. \quad (2.21)$$

The condition (2.21) makes that the comoving Hubble length $1/(aH)$, which is consider the most important characteristic scale of the expanding Universe¹⁴, is decreasing with time,

$$\frac{d}{dt} \left(\frac{1}{aH} \right) < 0. \quad (2.22)$$

This characteristic (2.22) is the key to solve the big bang model problems, as we going to see in this section. From the acceleration equation (2.8) the condition for inflation can be rewritten in terms of the material to drive the expansion, with $\Lambda = 0$ is founded,

$$\rho + 3p < 0. \quad (2.23)$$

In standard cosmology is assumed that ρ is always positive¹⁵, thus to satisfy the condition (2.23) is necessary a pressure p negative, which is independent of the Universe curvature. A wide range of behaviors satisfy the inflationary condition²⁵. The most classical is when $p = -\rho$, then the solution for the scale factor is

$$a(t) \propto \exp(Ht). \quad (2.24)$$

The inflation is a phenomenon at occurs at early Universe, which ends after certain time and later the convectional behavior of big bang theory continues²⁵. The big bang theory is not replaced by the inflation theory, on the contrary both theories work together to describe the early Universe.

2.2.1 Solution to the flatness problem

The flatness problem is solved with inflation, from the exponential growth at this epoch, see Eq. (2.24), then

$$|\Omega - 1| \propto e^{-2Ht}, \quad (2.25)$$

meaning that the differences between Ω and 1 decreases exponentially with time¹⁶. Comparing the density parameter at the beginning of the exponential inflation ($t = t_i$) with the density parameter at the end of inflation ($t = t_f = t_i + N/H$), is founded

$$|\Omega(t_f) - 1| = e^{-2N} |\Omega(t_i) - 1|, \quad (2.26)$$

where N is the number of e -foldings¹⁶. The above equations shows that at inflation epoch Ω is moved extremely closed to 1, if is close enough, then at the present time Ω will maintain the value very close to 1.²⁵ Inflation solves this problem fairly easy, since obtaining the sufficient of inflation to achieve this objective is not difficult.

2.2.2 Solution to the horizon problem

Prior the inflationary epoch the horizon distance $d_{hor}(t)$ at time t is defined by¹⁶

$$d_{hor}(t) = a(t)c \int_0^t \frac{dt}{a(t)}, \quad (2.27)$$

at the beginning inflation was

$$d_{hor}(t) = a_i c \int_0^{t_i} \frac{dt}{a(t/t_i)^{1/2}} = 2ct_i, \quad (2.28)$$

and at the end of the inflation was

$$d_{hor}(t_f) = a_i e^N c \left(\int_0^{t_i} \frac{dt}{a(t/t_i)^{1/2}} + \int_{t_i}^{t_f} \frac{dt}{a_i \exp[H(t - t_i)]} \right). \quad (2.29)$$

To large number of e -foldings the horizon size at the end of inflation comes to

$$d_{hor}(t_f) = e^N c (2t_i + H^{-1}), \quad (2.30)$$

meaning that at the epoch of exponential inflation the horizon size grow exponentially. The comoving Hubble length $1/(aH)$ suffers a great reduction during the inflation, causing that the region which would have visible before inflation started was much bigger than the region that is observed after inflation²⁵. But, after inflation the comoving Hubble length begins to grow faster. The condition to solve the horizon problem is

$$\int_{t_s}^{t_{dec}} \frac{dt}{a(t)} \gg \int_{t_{dec}}^{t_0} \frac{dt}{a(t)}, \quad (2.31)$$

ensuring that photons can travel much further before decoupling than it can afterwards²⁵. Hence the thermal equilibrium observed at present can be produced by the causal physics. According to Andrew R. Liddle¹⁴ the number of e -foldings should be $N \geq 60$ to achieve this solution to the horizon problem.

2.2.3 Solution to the monopole problem

According to Alan Guth²⁶ one of founders of inflation theory the monopole problem was one of the main reasons to develop the theory. The problem is solved from the fact that the energy density of the universe decreases very slowly ($\gtrsim a^{-2}$), during the inflation. In the other hand, the energy density of massive particles decreases much faster ($\sim a^{-3}$).¹⁷ If the monopoles was created before or during inflation, then the density of monopoles decrease exponentially, meaning that the probability of finding a single monopole at present is extremely low¹⁶.

2.2.4 Scalar fields in cosmology

Inflation is able to solve successfully the problems of the big bang model, but to obtain a inflationary epoch is necessary a peculiar material with negative pressure ($p < 0$). Such material is a scalar field $\phi(\vec{r}, t)$ that describes zero spin particles and usually is called *inflaton*¹⁴. The premise that the Universe is isotropic and homogeneous at

large scales allows to neglect the dependencies of \vec{r} of the scalar field to analyze just the temporal evolution of the field $\phi(t)$. Generally the scalar field have an associated potential energy $V(\phi)$ ¹⁶, which is the responsible to drive the exponential expansion of the universe¹⁷.

The inflationary field minimally coupled to gravity has the action

$$S = \int d^4x \sqrt{-g} \mathcal{L} = \int d^4x \sqrt{-g} \left[\frac{1}{2} \partial_\mu \phi \partial^\mu \phi - V(\phi) \right], \quad (2.32)$$

where \mathcal{L} is the Lagrangian density associated. In order to obtain the expressions to energy density and pressure, the corresponding energy-momentum tensor is defined by

$$T_{\mu\nu} = \partial_\mu \phi \partial_\nu \phi - g_{\mu\nu} \mathcal{L}. \quad (2.33)$$

Solving and running the indices of (2.33), the energy density and pressure of a homogeneous scalar field ($\nabla\phi = 0$) in the FRW metric are defined by

$$\rho_\phi = \frac{1}{2} \dot{\phi}^2 + V(\phi), \quad (2.34)$$

$$p_\phi = \frac{1}{2} \dot{\phi}^2 - V(\phi). \quad (2.35)$$

Note that the scalar field cannot have a equation of state that relates ρ and p because different values of energy density can be associated with different values of pressure, since the energy density is distributed in different ways between the kinetic and potential energy¹⁴.

Equations of motion

The equations of motion for a spatially flat universe ($k = 0$) are obtained replacing Eqns. (2.34) and (2.35) into the Friedmann equation (2.7) and fluid equation (2.9) giving

$$H^2 = \frac{1}{3M_{pl}^2} \left[V(\phi) + \frac{1}{2} \dot{\phi}^2 \right], \quad (2.36)$$

and

$$\ddot{\phi} + 3H\dot{\phi} = -\frac{dV}{d\phi}. \quad (2.37)$$

During the inflation the energy density and pressure satisfied the condition for inflation¹⁴, providing that $\dot{\phi}^2 < V(\phi)$. Therefore a flat potential is required to reach the sufficient amount of inflation¹⁷. The curvature term in the Friedmann equation can be neglected once the inflation stars.

2.3 Slow-roll approximation

The standard strategy to solve inflation with an scalar field is the **slow-roll approximation**¹⁴. The conditions that this strategy imposes are $\dot{\phi}^2 \ll V(\phi)$ and $\ddot{\phi} \ll V'(\phi)$ or equivalently $\ddot{\phi} \ll 3H\dot{\phi}$. From this conditions is observed that

inflation acquires a big dependence on the potential energy of the scalar field. The name of slow-roll becomes from the fact that the conditions make the scalar field slowly rolling down its potential¹⁵. The approximation reduce the equations (2.37) and (2.36) to

$$H^2 \simeq \frac{V(\phi)}{3M_{pl}^2}, \quad (2.38)$$

and

$$3H\dot{\phi} \simeq -V'(\phi). \quad (2.39)$$

The slow-roll approximation requires the the definition of two parameters,

$$\epsilon_V = M^2 \left(\frac{V'}{V} \right)^2, \quad (2.40)$$

and

$$\eta_V = M^2 \left(\frac{V''}{V} \right), \quad (2.41)$$

where ϵ_V and η_V are called the slow-roll parameters²⁷. The first measures the slope of the potential and the second the curvature²⁵. In order to the slow-roll approximation will be valid the the slow-roll parameters must accomplish two conditions which are

$$\epsilon_V \ll 1 \quad \text{and} \quad |\eta_V| \ll 1. \quad (2.42)$$

As we say this conditions are necessary for the slow-roll approximation, but they are not sufficient conditions¹⁴, since they only restrict the form of the potential and the scalar field can has a large velocity²⁵.

The condition for inflation can be directly related with the condition of the slow-roll , to observe this the condition of inflation can be rewritten as

$$\frac{\ddot{a}}{a} = \dot{H} + H^2 > 0. \quad (2.43)$$

Notice that the condition is easily satisfied if \dot{H} is positive. Otherwise is required

$$-\frac{\dot{H}}{H^2} < 1. \quad (2.44)$$

The above equation can be expressed with term of the slow-roll equation (2.40), obtaining

$$-\frac{\dot{H}}{H^2} \simeq \frac{M^2}{2} \left(\frac{V'}{V} \right)^2 = \epsilon_V, \quad (2.45)$$

meaning that the inflation is guaranteed if the slow-roll condition is reached ($\epsilon_V \ll 1$)¹⁴. The inflation models should reach this conditions, but also should be able to give a way of end the inflation. To achieve this the slow-roll parameters are usefully , since when ϵ_V and η_V are equal to the unity the inflation finishes¹⁷.

2.3.1 Amount of inflation

The amount of inflation is defined by the number of times that the scale factor a power expands during the inflation, typically this is called the number of e -foldings N , defined as

$$N(t) = \ln \frac{a(t_{end})}{a(t)}, \quad (2.46)$$

where t_{end} is the time at the end of the inflation. This can be expressed in terms of the scalar field potential:

$$N = \int_t^{t_{end}} H dt \simeq \frac{1}{M_{pl}} \int_{\phi_{end}}^{\phi} \frac{V}{V'} d\phi, \quad (2.47)$$

from this expression the amount of inflation can be calculated without solving the equations of motion for expansion¹⁴. From the CMB the number N that favorites inflation and solve the horizon and flatness problem should be $N \geq 60$ ²⁸.

2.4 Starobinsky inflationary model

The motivation to use the Starobinsky model of cosmic inflation born from the recent results from the Planck²⁹ mission and WMAP³⁰, where inflationary potentials with small values of $r < 0.11$ (tensor-to-scalar ratio) are favored including the Starobinsky potential³¹. This alternative scenario of inflation was develop with higher-derivative R^2 quantum gravity corrections³², meaning that the Ricci scalar R is the responsible to drive inflation from the beginning. The $R + R^2$ model, also called Starobinsky model is defined by the action

$$S = \frac{M^2}{2} \int d^4x \sqrt{-g} \left(R + \frac{1}{6m^2} R^2 \right), \quad (2.48)$$

where m is the inflation mass and is the only parameter. Later, the expression (2.48) is rewritten in the "linear" representation³³, obtaining

$$S = \int d^4x \sqrt{-g} \left(\frac{M^2}{2} R + \frac{1}{m} R\psi - 3\psi^2 \right), \quad (2.49)$$

where is observed that integrating out ψ , results in reverting to original theory. By means of the conformal transformation given by³⁴

$$g_{\mu\nu} = f'(R) g_{\mu\nu} = \left(1 + \frac{2\psi}{mM^2} \right)^{-1} g_{\mu\nu}, \quad (2.50)$$

the equivalent scalar field version of the Starobinsky model is obtained,

$$S = \int d^4x \sqrt{-g} \left[\frac{M^2}{2} R - \frac{1}{2} \partial_\mu \phi \partial^\mu \phi - \frac{3}{4} M_{pl}^4 m^2 \left(1 - e^{-\sqrt{2/3} \phi / M_{pl}} \right)^2 \right]. \quad (2.51)$$

From the above expression is observed that in the right part of the expression the Starobinsky potential appears for first time, which is rewritten as

$$V(\phi) = \frac{3}{4} M^2 \left(1 - e^{-\sqrt{2/3} \phi} \right)^2, \quad (2.52)$$

where $M = 1.13 \times 10^{-5} M_{pl}^{35}$ and $M_{pl} = 1$, for the purposes of this work.

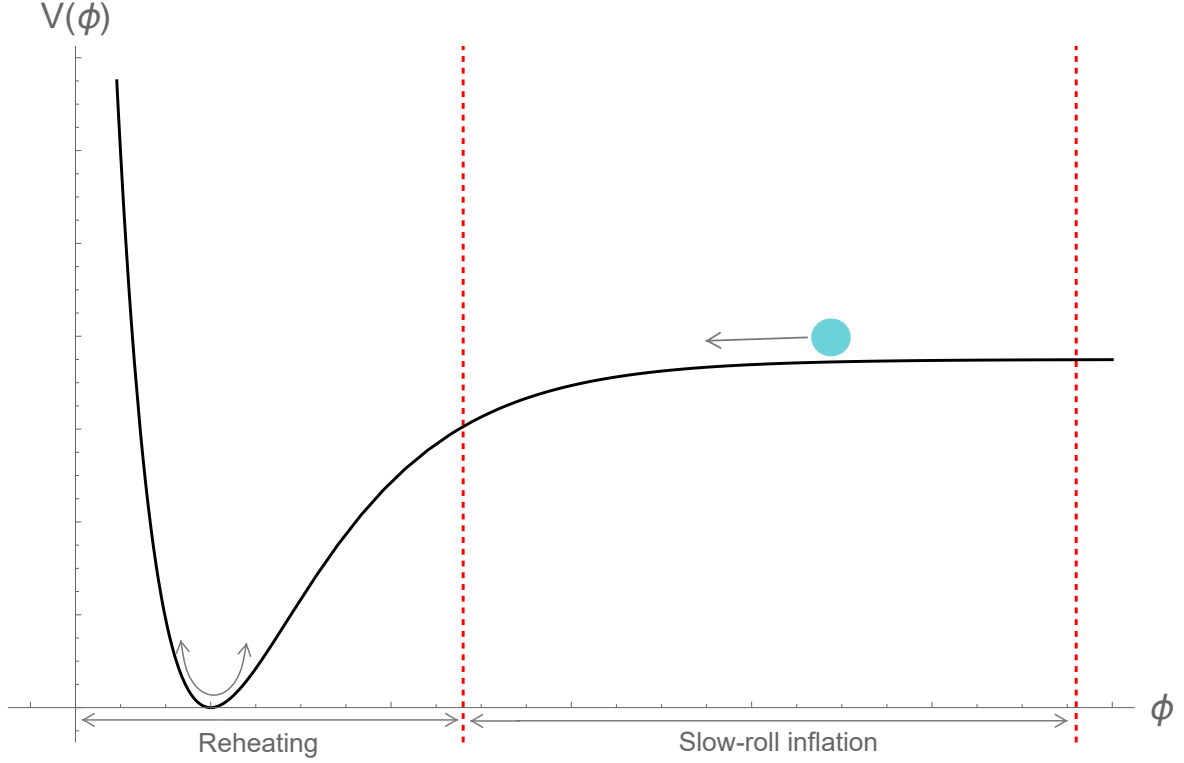


Figure 2.1: Starobinsky potential $V(\phi) = \frac{3}{4}M^2(1 - e^{-\sqrt{2/3}\phi})^2$ for inflation, the red dashed delimit the regions of reheating and slow roll inflation. (Adapted from: R. Casadio)³⁶.

From Fig 2.1 is observed that the scalar potential is non-negative and stable and has a minimum at $\phi = 0$ corresponding to the Minkowski vacuum³⁷. The scalar field potential $V(\phi)$ increases exponentially for $\phi < 0$, and reach a constant value $\frac{3}{4}M^2$ for $\phi \rightarrow \infty$ resulting in a plateau of positive height that results in the slow-roll of the inflation³⁷.

2.4.1 Equations of motion with Starobinsky model

The scalar potential of the energy density (2.34) and pressure equation (2.35) can be replaced by the Starobinsky potential, obtaining

$$\rho_\phi = \frac{1}{2}\dot{\phi}^2 + \frac{3}{4}M^2(1 - e^{-\sqrt{2/3}\phi})^2 \quad \text{and} \quad p_\phi = \frac{1}{2}\dot{\phi}^2 - \frac{3}{4}M^2(1 - e^{-\sqrt{2/3}\phi})^2. \quad (2.53)$$

The Friedmann equation (2.36) and the fluid equation (2.37) with the Starobinsky potential are expressed as

$$H^2 = \frac{1}{3M_{pl}^2} \left[\frac{3}{4} M^2 (1 - e^{-\sqrt{2/3}\phi})^2 + \frac{1}{2} \dot{\phi}^2 \right], \quad (2.54)$$

and

$$\ddot{\phi} + 3H\dot{\phi} = -\sqrt{\frac{3}{2}} M^2 e^{-\sqrt{2/3}\phi} (1 - e^{-\sqrt{2/3}\phi}). \quad (2.55)$$

Remember that the slow-roll approximation is used to describe the inflation, meaning that the above equations are reduced to

$$H^2 \simeq \frac{M^2}{\sqrt{3}} (1 - e^{-\sqrt{2/3}\phi}), \quad (2.56)$$

and

$$3H\dot{\phi} \simeq -2\sqrt{\frac{2}{3}} M^2 (1 - e^{-\sqrt{2/3}\phi}). \quad (2.57)$$

Notice that above expressions are dependent of the scalar field, its first derivative and the scale factor. The scalar field solution for the Friedmann equation is³⁸

$$\phi_{sr}(t) \simeq \sqrt{\frac{3}{2}} \ln \left[\frac{1}{9} (e^{-\sqrt{2/3}\phi_{mi}} - 4\sqrt{3}M^2 t) \right], \quad (2.58)$$

and the solution to the scale factor is defined by

$$a_{sr}(t) \simeq \text{Exp} \left[\frac{M^2 t}{\sqrt{3}} - \frac{3}{4} \ln (e^{-\sqrt{2/3}\phi_{mi}}) + \frac{3}{4} \ln \left(e^{-\sqrt{2/3}\phi_{mi}} - \frac{4M^2 t}{3\sqrt{3}} \right) \right]. \quad (2.59)$$

In Chapter 3 the scalar field solution are presented in term of e -folding number N , for this the solution is obtained from the relation (2.47), in order to express the tensor and scalar spectra indices in terms of N .

2.5 The CMB angular power spectrum

2.5.1 Primordial cosmic fluctuations

Inflation becomes a popular theory not only for solving the problems of the standard Big-Bang model, also provide a explanation for the production of the first density perturbations which are consider as the "seeds"³⁹ for the large scale structure and the anisotropies that are observed in the CMB at present. These fluctuations arises from the quantum fluctuations in the inflaton field about the vacuum fluctuation¹⁴, driving the fluctuations to scales much larger than the Hubble horizon¹⁵. Then, the amplitude of the perturbations can not be modified and is say that they are frozen³⁹.

The inflationary field produce two types of fluctuations, the scalar or curvature perturbations that are related with the matter in the Universe and are responsible of the large scale structure observed today, and the tensor perturbations that are associated with the generation of primordial gravitational waves¹⁵. Despite, the tensor perturbations have no effect on the structure formation, these are important in the CMB anisotropies that are observed today⁴⁰.

2.5.2 Temperature anisotropies

The Cosmic Microwave Background (CMB) shows an average temperature (thermal equilibrium) $T = 2.72K$ over a large range of frequencies⁴¹. However, exist small temperature anisotropies at the $O(10^{-5})$ which come from the primordial perturbations⁴². This small deviations in the temperature, are defined by a dimensionless quantity⁴³

$$\Theta(\hat{n}) = \frac{T(\hat{n}) - \langle T \rangle}{\langle T \rangle}, \quad (2.60)$$

where T is the temperature and \hat{n} is the direction in the sky in comoving polar coordinates $\hat{n} = (\theta, \phi)$.

The temperature fluctuations are projected in a 2D spherical surface, for this reason usually the temperature field is expanded using spherical harmonics. The spherical harmonics form a complete orthonormal set on the unit sphere⁴³ and are defined as

$$Y_{lm} = \sqrt{\frac{2\ell + 1(\ell - m)!}{4\pi(\ell + m)!}} P_{\ell}^m(\cos\theta)e^{im\phi}, \quad (2.61)$$

where P_{ℓ}^m are the Legendre polynomials, the indices $\ell = 0, 1, \dots, \infty$ and $-\ell \leq m \leq \ell$. Formally ℓ is called the multipole moment and are related with a given angular scale in the sky α by $\alpha = \pi/\ell$ (in degrees). Later the temperature fluctuations field is expanded using the functions

$$\Theta(\hat{n}) = \sum_{\ell=0}^{\infty} \sum_{m=-\ell}^{\ell} a_{lm} Y_{lm}(\hat{n}), \quad (2.62)$$

where

$$a_{lm} = \int_{\theta=-\pi}^{\pi} \int_{\phi=0}^{2\pi} \Theta(\hat{n}) Y_{lm}^*(\hat{n}) d\Omega. \quad (2.63)$$

From this, the power spectrum of the fluctuations C_{ℓ}^T can be defined as the variance of the harmonic coefficients

$$\langle a_{lm} a_{l'm'}^* \rangle = \delta_{\ell\ell'} \delta_{mm'} C_{\ell}^T, \quad (2.64)$$

where the delta functions $\delta_{\ell\ell'}$ and $\delta_{mm'}$ arises from the isotropy of Universe⁴³. The number of independent m modes are limited to $(2\ell + 1)$ of these for each multipole. The power spectrum can be rewritten as

$$C_{\ell}^T = \frac{1}{2\ell + 1} \sum_{m=-\ell}^{\ell} \langle |a_{lm}|^2 \rangle. \quad (2.65)$$

From the above expression is notable that an error in the estimation of any given C_{ℓ}^T of $\Delta C_{\ell}^T = \sqrt{2/(2\ell + 1)}$, meaning that our estimations in the average value is dependent of how many points we have on the sample. This is called the cosmic variance⁴³. From the inflation theory, the temperature fluctuations are Gaussian with mean zero and variance given by C_{ℓ}^T , meaning that the power spectrum characterize the statistics of the temperature fluctuations field⁴³.

Usually in the temperature power spectrum C_{ℓ}^T is observed that the multipole moment begins in $\ell = 2$ and goes to ℓ_{max} . The reason to exclude the first two multipole moments ($\ell = 0$ and $\ell = 1$) is that the first ($\ell = 0$) is simply the

average temperature over the whole sky⁴³ and by the definition (2.62) it should average to zero. The second dipole term ($\ell = 1$) is affected by the our own motion across space⁴³, since the blueshift and redshift effect of the coming photons creates an anisotropy at this scale which "dominates over the intrinsic cosmological dipole signal"⁴³. High values of multipole moments ℓ are related with the resolution of the data, as is observed in Figure 2.2

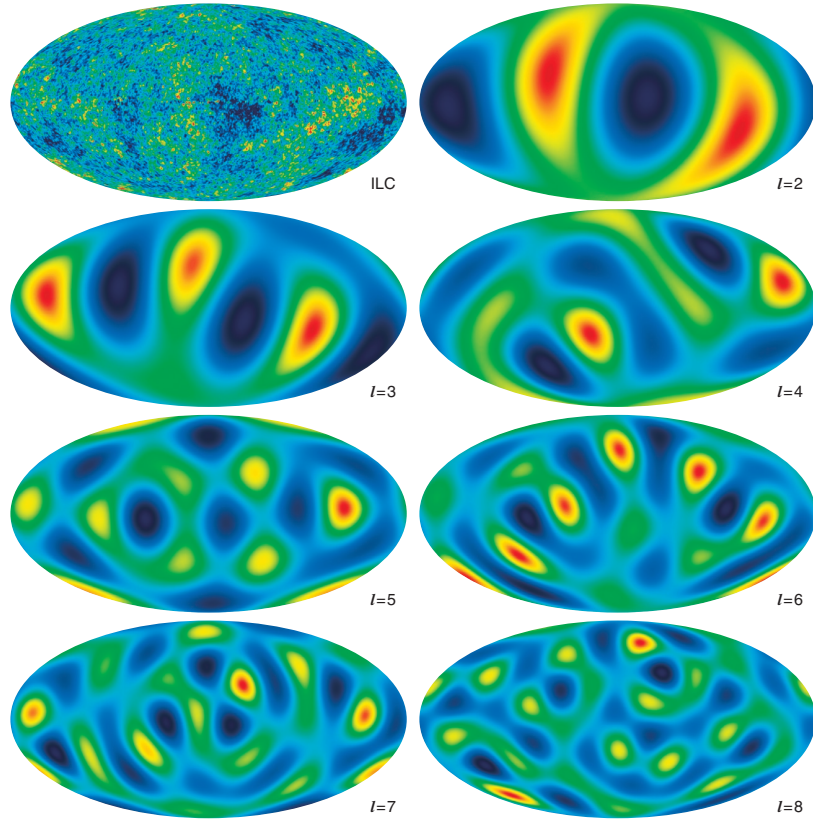


Figure 2.2: Maps of power spectrum modes $\ell = 2$ to $\ell = 8$ computed from full-sky fits to the ILC map, shown at top left. (Credit: NASA / WMAP Science Team)⁴⁴.

2.5.3 The power spectrum in terms of tensor and scalar spectral index

The power spectrum is a valuable tool to characterize the properties of the fluctuations of the inflation field. The primordial spectra of scalar and tensor perturbations are expanded around a pivot scale⁴⁵ k that is usually represented by k_* , and are defined by

$$\mathcal{P}_{\mathcal{R}}(k) = A_s \left(\frac{k}{k_*} \right)^{n_s - 1 + \frac{1}{2} dn_s / d \ln k \ln(k/k_*) + \frac{1}{6} d^2 n_s / d \ln k^2 (\ln(k/k_*))^2 + \dots}, \quad (2.66)$$

$$\mathcal{P}_t(k) = A_t \left(\frac{k}{k_*} \right)^{n_t + \frac{1}{2} \frac{dn_t}{d \ln k} \ln(k/k_*) + \dots}, \quad (2.67)$$

where A_s , A_t is the scalar, tensor amplitude respectively and n_s , n_t , $dn_s/d \ln k$, $dn_t/d \ln k$, and $d^2 n_s/d \ln k^2$ are the scalar, tensor spectral index, the running of the scalar, spectral index, and the running of the running of the scalar spectral index, respectively. With the primordial spectra of the scalar and tensor perturbations defined, the tensor-to-scalar ratio is given by

$$r = \frac{\mathcal{P}_t(k_*)}{\mathcal{P}_R(k_*)}. \quad (2.68)$$

In the slow-roll regime the scalar and tensor power spectra for a single field model is defined by⁴⁶

$$\mathcal{P}_R(k) \simeq \frac{2}{3\pi M_{pl}^6} \frac{V^3}{V'^2}, \quad (2.69)$$

and

$$\mathcal{P}_t(k) \simeq \frac{16V}{3\pi M_{pl}^4}, \quad (2.70)$$

in which is considered the power spectra up to the lowest powers of the slow roll parameters⁴⁶. Later, using the relation

$$\frac{d}{d \ln k} \simeq -M_{pl}^2 \frac{V'}{V} \frac{d}{d\phi}, \quad (2.71)$$

obtained from the power spectra expansion, is possible to compute the scalar and tensor spectral indices and their corresponding running terms in terms of the slow-roll parameters ϵ_V and η_V , obtaining:

$$n_t(k) \simeq -2\epsilon_V, \quad (2.72)$$

$$n_s(k) \simeq 1 - 6\epsilon_V + 2\eta_V, \quad (2.73)$$

$$\frac{dn_t(k)}{d \ln k} \simeq 4\eta_V \epsilon_V - 8\epsilon_V^2, \quad (2.74)$$

$$\frac{dn_s(k)}{d \ln k} \simeq 16\eta_V \epsilon_V - 24\epsilon_V^2 - 2\xi_V^2, \quad (2.75)$$

$$\frac{d^2 n_s(k)}{d \ln k^2} \simeq 192\epsilon_V^3 - 192\epsilon_V^2 \eta_V + 32\epsilon_V \eta_V^2 + 24\epsilon_V \xi_V^2 - 2\eta_V \xi_V^2 - 2\varpi_V^3, \quad (2.76)$$

where

$$\xi_V^2 = \frac{M^4 V'(\phi) V''''(\phi)}{V^2(\phi)}, \quad \text{and} \quad \varpi_V^3 = \frac{M^6 V'(\phi)^2 V(\phi)''''}{V(\phi)^3}. \quad (2.77)$$

The tensor-scalar ratio is defined in terms of slow-roll parameters, by

$$r = \frac{\mathcal{P}_t(k_*)}{\mathcal{P}_R(k_*)} \simeq 16\epsilon_V \simeq -8n_t. \quad (2.78)$$

Chapter 3

Results & Discussion

The CMB temperature (TT) power spectrum C_ℓ^T shows the temperature fluctuations in the cosmic microwave background at different angular scales in the sky⁴⁷. The CMB temperature power spectrum can be divided and analyzed in three parts, each part dominated by a different physical process of the early Universe. Those regions correspond to: (a) Angular scales larger than the causal horizon size at decoupling ($\ell < 90$). This part is called the ‘‘Sachs-Wolfe plateau’’¹¹.(b) The acoustic peak region with multipole moment between 90 and 900 ($90 < \ell < 900$) and (c) The Silk damping region with multipole moment bigger than 900⁴⁸ ($\ell > 900$).

In this chapter is presented the CMB temperature (TT) power spectrum obtained with a Starobinsky inflationary potential $V = \frac{3}{4}M^2(1 - e^{-\sqrt{2/3}\phi})^2$ in a slow-roll approximation, the spectrum is compared with the recent data reported by the Planck’s satellite. First, the entire TT power spectrum is presented and analyzed. Subsequently, each of the three part named above is presented and analyzed individually. Finally, how the scalar and tensor spectral indices and their corresponding running terms with the Starobinsky potential in the slow-roll approximation were obtained and used in the CAMB¹³ code to obtain the CMB temperature power spectrum.

3.1 Angular power spectrum with Starobinsky potential into a slow-roll approximation

The cosmic microwave background (CMB) radiation plays a important role in cosmology, since give us a clear picture of the early Universe. Later, the discovery of temperature anisotropies of the CMB by the Cosmic Background Explorer (COBE) satellite⁴⁹, help to construct and improve models that describe the evolution of the Universe. These anisotropies can be defined as a point to point variations of temperature across the sky on the CMB¹ and are at 10^{-5} level⁴². The angular TT power spectrum C_ℓ^T help us to studying those anisotropies at different angular scales.

As we saw in the last section Chapter (2), the definition of the power spectrum becomes from the spherical harmonic expansion:

$$\Theta(\hat{n}) = \sum_{\ell m} \Theta_{\ell m} Y_{\ell m}(\hat{n}), \quad (3.1)$$

where the index ℓ corresponds to anisotropies at scale $180/\ell^{42}$. The importance of the TT power spectrum is that help to understand and describe the physical processes in the early Universe, also is used to improve the estimation of different cosmic parameters⁵⁰.

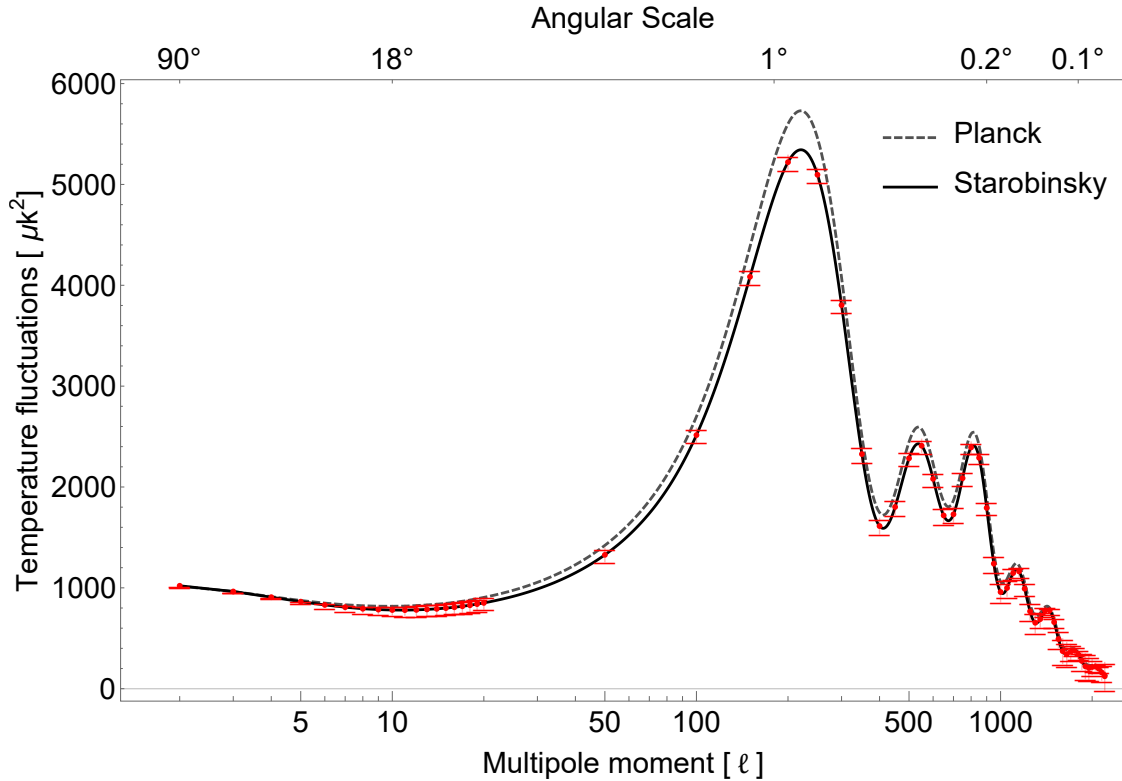


Figure 3.1: In dashed gray line the CMB temperature power spectrum reported from Planck satellite⁴⁷, in black solid line the CMB temperature power spectrum obtained with Starobinsky potential in a slow-roll approximation, with their respective uncertainties (red) increased by a factor of 1000. The multipole moment (ℓ) and angular scale in logarithmic scale, the temperature fluctuations in micro kelvins (μk^2).

The interest in the CMB angular power spectrum increases in the last century, many mission and projects studied the CMB anisotropies, but three missions are the most relevant. First, the COBE satellite launched in 1989, later his successor the Wilkinson Microwave Anisotropy Probe (WMAP) satellite launched in 2001⁵¹. Later in 2009, the Planck satellite launched by ESA¹ recollected the data from the CMB anisotropies, giving in 2013 an accuracy angular power spectrum that agrees with the actual Λ CDM model¹.

We compare our TT power spectrum obtained from our model (Starobinsky model) with the Planck satellite data, since the data reported by Planck satellite is more accurate and recent than the COBE and WMAP data. The com-

parison between both TT power spectrum are presented in Figure 3.1. We can notice that the TT power spectrum that we obtain compared with the Planck satellite TT power spectrum looks similar in all the regions. But, the power spectrum that we obtained shows lower values almost in the whole range. The bigger differences are presented in the acoustic peak region ($90 < \ell < 900$), since the Starobinsky model shows smaller temperature fluctuations, resulting in a smaller peaks than the Planck satellite data.

As we saw the TT power spectrum shows how the temperature anisotropies or "fluctuations" are distributed across the sky. The Starobinsky model with an slow-roll approximation give us a TT power spectrum that shows lower temperature anisotropies at almost every multipole moment ($\ell \geq 7$), this behavior are related with the values of cosmic parameters, as we show in the next sections.

3.1.1 Relative error and percentage of relative error

In general a good cosmological model can be judged by how well it can reproduce the CMB power spectrum observed¹.

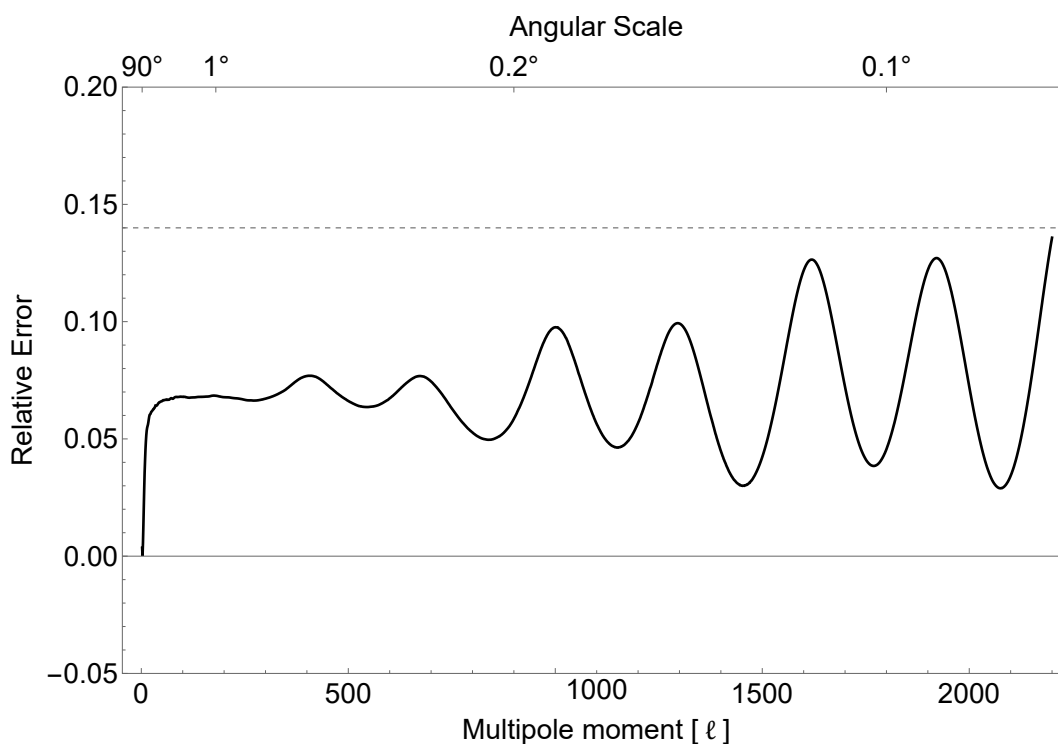


Figure 3.2: Relative error of TT power spectrum obtained from Starobinsky model with slow-roll approximation. The values of Planck satellite are tacked as the real values.

As is showed in Figure 3.1 the Starobinsky model reproduce a "good" CMB power spectrum, since the values of the temperature fluctuations are very related with the values that we observe from the Planck satellite, this is confirmed in Figure 3.2 and Figure 3.3, where is showed the relative error and the the relative error in percentage respectively, between both spectrum.

The relative error oscillates between 0 and 0.15 in the whole spectrum Figure 3.2 and the percentage of relative

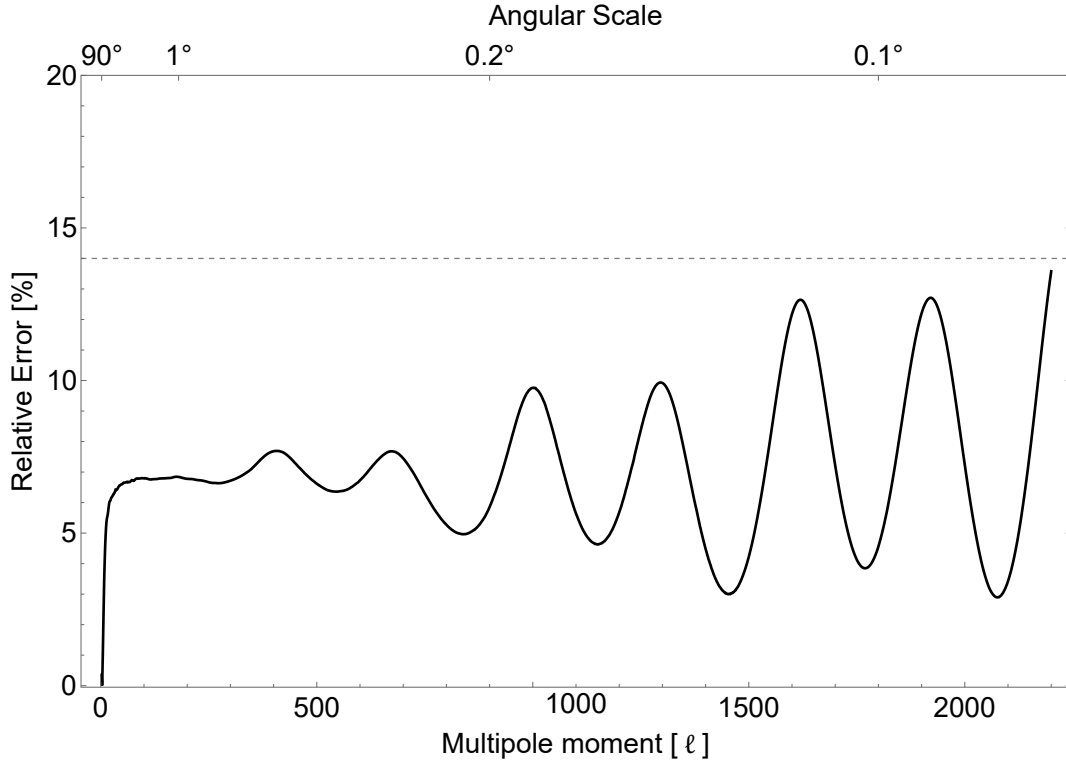


Figure 3.3: Percentage of relative error of TT power spectrum obtained from Starobinsky model with slow-roll approximation. The values of Planck satellite are tacked as the real values.

error show values lower than 25% Figure 3.3 , reaffirming that the Starobinsky model reproduce an accurate TT power spectrum and the model is capable to describe the evolution of our Universe. The Sachs-Wolfe Plateau region and Acoustic Peak region shows slower oscillations of relative error than the Silk Damping region. Therefore, the biggest values of relative error observed are in the Silk Damping region ($\ell > 900$), more precisely at the end of the TT power spectrum ($\ell > 1500$), meaning that at high multipole moment the uncertainty of our model increases.

As we say, in the Acoustic Peak region the difference in the temperature fluctuations are bigger between the Starobinsky model spectrum and the Planck satellite spectrum, but the small values of relative error and percentage of relative error ($< 12\%$) indicates that this differences are not big enough to reject the results with our model in that region. The qualitatively and quantitatively analysis shows that the Starobinsky inflation model describes very well

the temperature fluctuations that are presented in the early Universe.

3.2 “Sachs-Wolfe plateau” region ($\ell < 90$)

The “Sachs-Wolfe plateau” region Figure 3.4 correspond to large angular scales ($\theta > 2$). In this TT spectrum region the primordial temperature fluctuations are presented⁴⁸. The temperature power spectrum shape in this region is mainly dominated by the Sachs-Wolfe effect and the early integrated Sachs-Wolfe effect⁵². The Sachs-Wolfe effect refers to the spatial fluctuations in the gravitational potential at the time of decoupling that caused a shift in the frequency of photons, varying their temperature⁵². The early integrated Sachs-Wolfe effect is responsible of the evolution of gravitational potentials, which changed the energy of photons between recombination and present⁵².

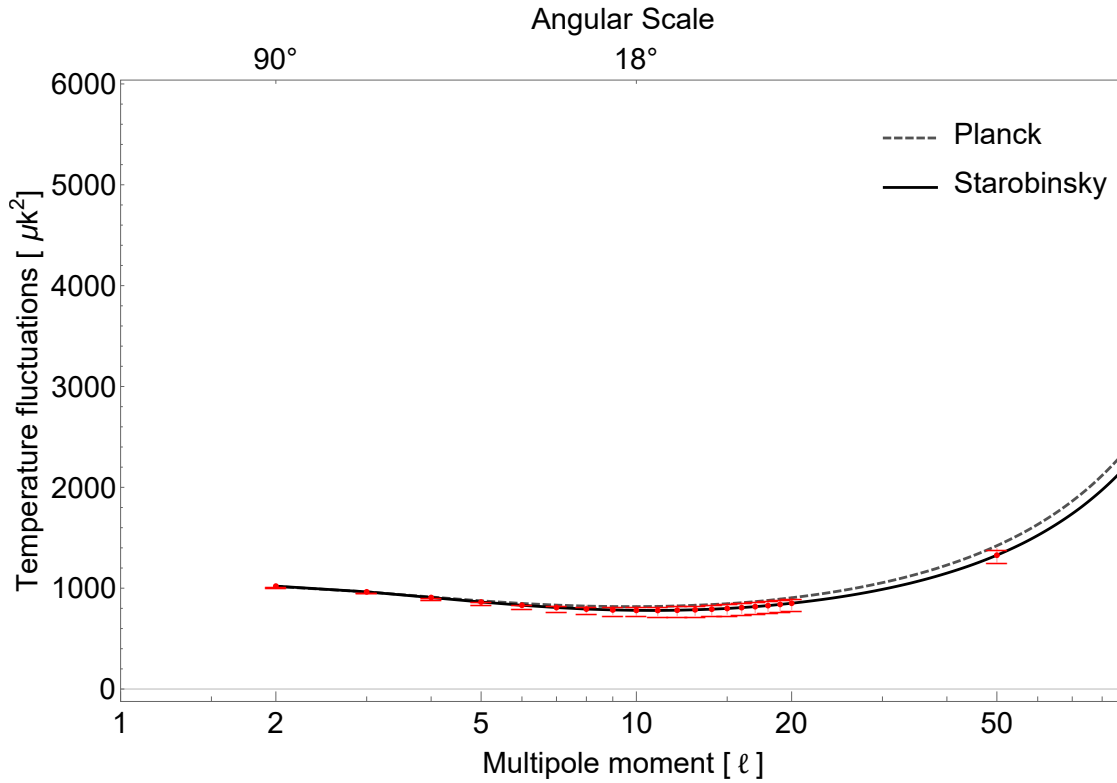


Figure 3.4: “Sachs-Wolfe plateau” region obtained from Starobinsky potential with slow-roll approximation in black solid line with uncertainties increment by a factor of 1000. “Sachs-Wolfe plateau” region reported by Planck satellite in gray dashed line.

The TT power spectrum reproduced by the Starobinsky model are qualitatively the same at large scales ($\theta \geq 35$) as the TT power spectrum observed by the Planck satellite. In the other hand at small angular scales ($\theta < 35$) the TT power spectrum that we reproduced begins to show lower temperature fluctuations. At analysing the entire region we observe in Figure 3.2 and Figure 3.3 the smaller values of relative error (< 7) meaning that the Starobinsky model describes with high accuracy the primordial fluctuations observed in the CMB.

The TT power spectrum reproduced in this region by the Starobinsky model in a slow-roll approximation describes a inflationary epoch. The Planck satellite provides strong support for the inflationary models¹, meaning that our model is good candidate to describe the evolution of early Universe. The behavior of this region evolved first linearly and then non-linearly, this may indicate that our Universe must have started as a very homogeneous substance.

3.3 “Acoustic Peak” region ($90 < \ell < 900$)

The "Acoustic Peak" region presented in Figure 3.5 is of high interest since the first and the most higher peak are presented in this region, also the peaks and troughs are directly related with the values of cosmic parameters⁵³. The "Acoustic Peak" region represent the temperature fluctuations that interact with the gravitational potential produced by dark matter⁴⁸. The name of this region comes from the presence of "acoustic oscillations" that are produced by the high densities of dark matter that attracted photons and baryons to a gravitational potential well and compressed them, until the pressure of the the fluid composed by photons and baryons was highly enough to counteract gravity and drive the fluctuations apart; then the gravity could again compress the fluid and enhance the high densities⁵². This region are composed by three peaks and two troughs. their position and amplitude that Starobinsky model and Planck satellite reports are presented in Table 3.1. The first peak in the TT power spectrum is attributed to the first mode of oscillating sound waves in the coupled photon-baryon fluid, reaching the maximum temperature and density as the Universe recombines¹. The second peak are related with a "rarefaction" phase of an acoustic wave, meaning that the acoustic wave can compress and rarify at the same conformal time that it takes the plasma to compress over the acoustic horizon⁴⁰. The third peak appears from the second harmonic of the first peak⁴⁸.

The position (multipole moment ℓ) and amplitude (temperature fluctuations μk^2) are directly related, with: the age of the Universe, the mass density Ω_m , the baryon density $\Omega_b h^2$, and the scalar index n_s ⁴⁸. The position of the first peak is directly correlated with the age of the Universe⁵³. The Starobinsky model reproduces the first peak at 221ℓ and Planck satellite report the first peak at 220ℓ , meaning that the age of the universe that Starobinsky model describe should be different. The age of the universe that report Planck satellite in 2018 results is 13.797 ± 0.023 Gyr¹ and our model give us an age of 13.798 ± 0.007 Gyr, as is showed in Table 3.2, confirming our assumption. According to Lyman A. Page of Princeton university and collaborator of the WMAP mission: "increasing Ω_m decreases the first peak height"⁴⁸, as is observed in Figure 3.5 and Table 3.1 the Starobinsky model give us a lower value of amplitude in the first peak. The amplitude of the second peak depends of the same parameters (Ω_m , $\Omega_b h^2$, n_s) as the first peak⁴⁸, meaning that higher values of Ω_m affects the height of the second peak. Similar behavior is presented by the baryon density, since at increasing the baryon density $\Omega_b h^2$ decreases the amplitude of the second

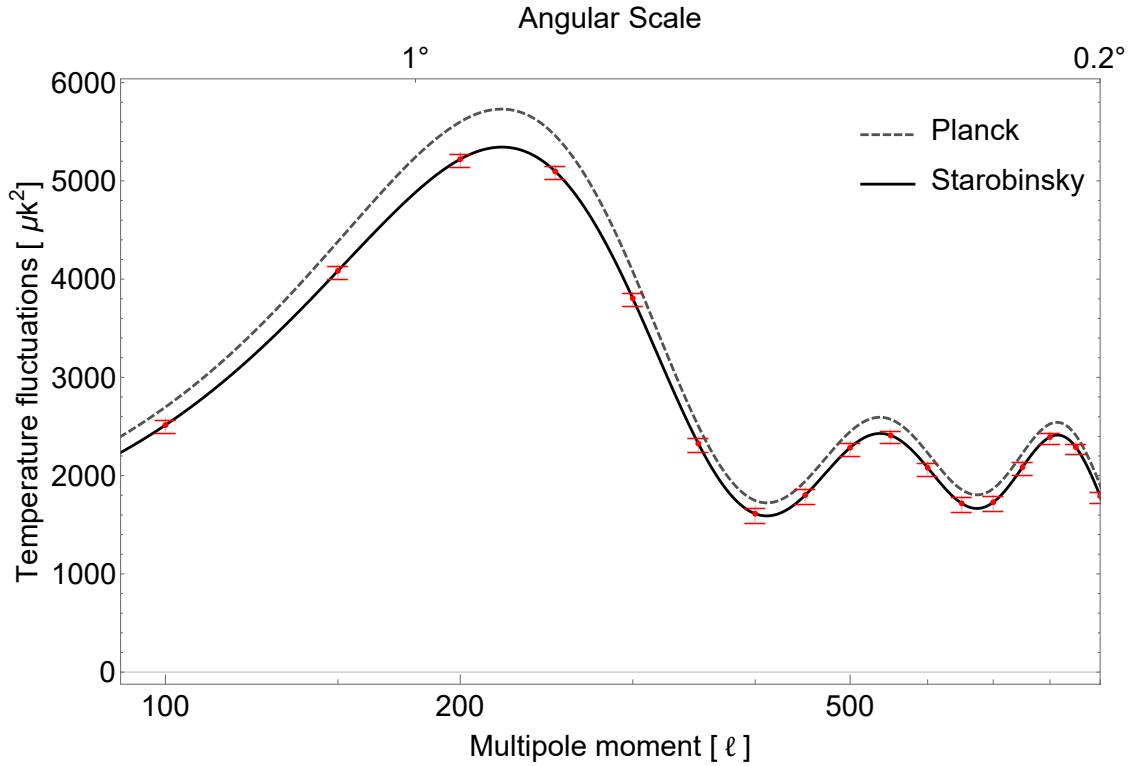


Figure 3.5: Comparison between the Acoustic Peak region obtained from Starobinsky model and the Acoustic Peak region reported by Planck satellite. The Starobinsky model data in black solid line, with uncertainties increases by a factor of 1000. Planck satellite data in gray dashed line.

and third peak in this region⁴⁸. From this, we can assume that our model reports higher values of mass density Ω_m and baryon density $\Omega_b h^2$. This assumption is confirmed, since our model give as a value of $\Omega_m \approx 0.3158 \pm 0.001$ and $\Omega_b h^2 \approx 0.02238 \pm 0.00044$ Table 3.2 ,while the Planck results reports a value of $\Omega_m \approx 0.3153 \pm 0.007$ and $\Omega_b h^2 \approx 0.02237 \pm 0.00015$ ¹. Lyman A. Page explains that at increasing the baryon density, the inertia in the photon-baryon fluid increases, resulting in lower amplitudes in the second and third peak of the "Acoustic region"⁴⁸. In the other hand, the increase of mass density decrease the amplitude of the first peak due to the additional mass loading of the baryon-photon fluid⁴⁸.

The dependence of n_s in the amplitude of the peaks comes from the overall slope of the CMB power spectrum, meaning that increasing n_s increases the height of the second peak relative to the first peak⁴⁸. The value of n_s Table 3.2 and the differences in the amplitude of the first and second peak that we reproduce with the Starobinsky model Table 3.1 agrees with this statement.

Extremum	Multipole [ℓ]	Amplitude [μk^2]
Starobinsky model		
Peak 1	221	5343.62 \pm 0.067
Trough 1	411	1590.24 \pm 0.076
Peak 2	537	2428.63 \pm 0.063
Trough 2	674	1665.86 \pm 0.076
Peak 3	814	2412.49 \pm 0.050
Planck Satellite		
Peak 1	220	5730.14 \pm 39
Trough 1	411	1722.75 \pm 20
Peak 2	537	2593.81 \pm 23
Trough 2	674	1804.44 \pm 14
Peak 3	814	2542.08 \pm 17

Table 3.1: Peaks of the CMB TT power spectra in the "Acoustic Peak" region recreated by the Starobinsky model and reported by Planck satellite¹.

To summarize this section, the TT power spectrum that we reproduce with the Starobinsky model in a slow-roll approximation shows that lower values in the amplitude of the peaks are correlated with different values of some cosmic parameters (Age , Ω_m , $\Omega_b h^2$ and n_t) and small changes in the physical process that dominates this region. The values of: age of Universe, matter density Ω_m , baryon density $\Omega_b h^2$ and scalar index n_t , obtained from Starobinsky model are presented in Table 3.2. The different value in the age of the Universe (13.798 ± 0.007) that we obtain is attributed from the different location ($\ell = 221$) of the first peak in the TT power spectrum. The amplitude of the first peak in the TT power spectrum that we reproduce shows a smaller value than the amplitude of the first peak that Planck satellite reports, obtaining higher values of matter density, meaning that additional mass was loaded in the photon-baryon fluid at recombination. Also, the smaller amplitude shows a smaller temperature limit at recombination. The smaller amplitudes of the second and third peak that our model shows are attributed to the increment of inertia in the photon-baryon fluid due to the increment in the baryon density. Finally, the higher value of scalar index n_s influence in the amplitude of the three peaks present in this region, since n_s comes from the overall slope of the CMB power spectrum.

3.4 "Silk Damping" region ($\ell > 900$)

This region is the result of approach the epoch of decoupling, when the diffusion of photons in the primordial plasma occurs⁵⁴. This effect causes that the anisotropies are exponential damped, making the universe itself more uniform⁵⁵. The shape of the damping tail of the TT power spectrum is sensitive to changes in baryon density $\Omega_b h^2$, increasing $\Omega_b h^2$ makes that the damping tail shifts to smaller angular scales⁵⁶. The damping tail obtained from our

Cosmic Parameter	Symbol	Starobinsky	Planck
Age of Universe (Gyr)	Age	13.798 ± 0.007	13.797 ± 0.023
Matter density	Ω_m	0.3158 ± 0.0015	0.3153 ± 0.0073
Baryon density	$\Omega_b h^2$	0.02238 ± 0.0004	0.02237 ± 0.0001
Scalar index	n_s	0.9653 ± 0.0004	0.9649 ± 0.0042

Table 3.2: Cosmic parameters obtained from the Starobinsky model compared with the cosmic parameters reported by Planck¹.

model shows a small shift in at smaller angular scales ($\ell > 1500$), see Figure 3.6, also the higher value of $\Omega_b h^2$, see Table 3.2, showing that our model agrees with theory. The shift on the damping tail at increasing $\Omega_b h^2$ is attributed to a photon-baryon fluid more tightly coupled at recombination making the mean free path of photons shorter⁵⁶.

Even though this region shows qualitatively almost a identical TT power spectrum between our model and the data

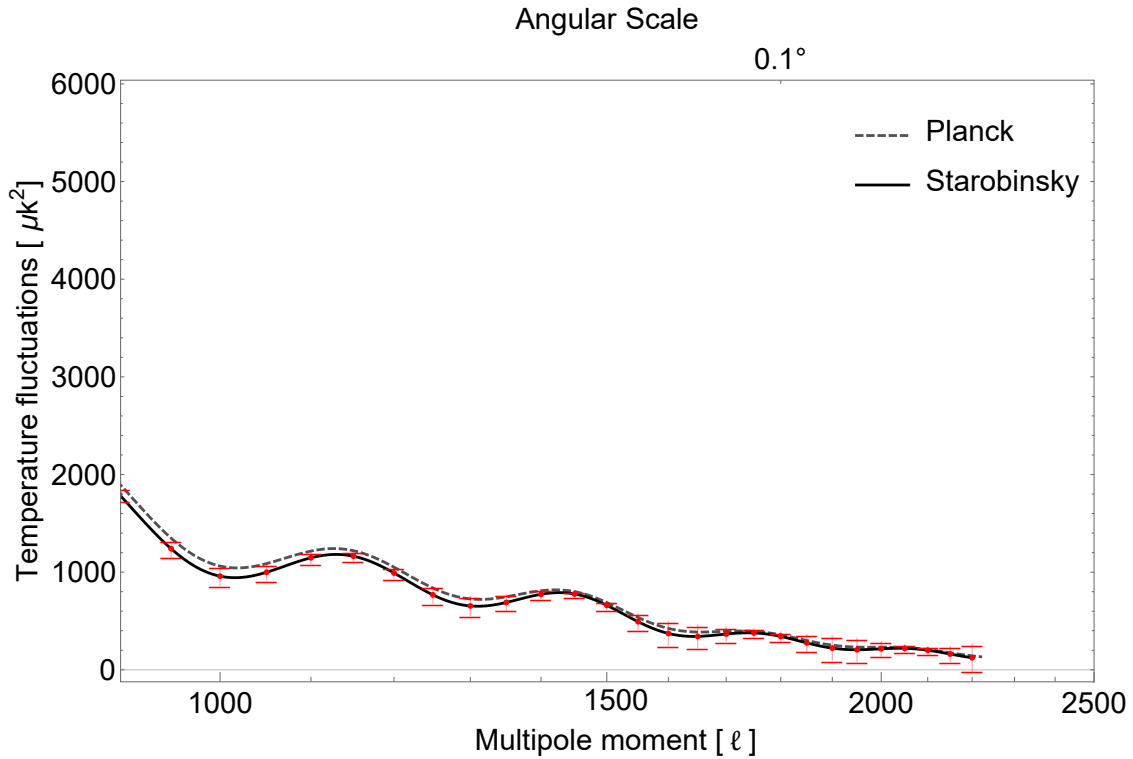


Figure 3.6: Silk Damping region reproduced by the Starobinsky potential with slow-roll approximation black solid line, uncertainties in red and increment by a factor of 1000. Silk Damping region reported by the Planck satellite in gray dashed line.

observed Figure 3.6, the bigger relative error Figure 3.2 of the entire TT power spectrum is presented in this region. From this we can deduce that not only our recreated Silk Damping region has a considerable uncertainty (> 10), also this region is observed with high accuracy from Plank satellite.

3.5 Methodology

In order to obtain the results presented in Chapter 3, the scalar and tensor spectral indices, their respective running values and the tensor-to-scalar ratio was computed to subsequently use the CAMB code. First, to get scalar and spectral indices with the Starobinsky potential $V = \frac{3}{4}M^2 \left(1 - e^{-\sqrt{2/3}\phi}\right)^2$ in a slow-roll approximation, the inflation field ϕ in terms of e -folding number N should be found. For a single field model, N is defined as

$$N(\phi) = \int_t^{t_e} H(t)dt = M_{pl}^{-2} \int_{\phi_e}^{\phi} \frac{V}{V'} d\phi, \quad (3.2)$$

where t_e and ϕ_e denotes the end of inflation. At solving the integral equation the approximated inflation field obtained from the Starobinsky potential is defined as

$$\phi(N) \simeq \sqrt{\frac{3}{2}} \ln \frac{4N}{3}. \quad (3.3)$$

As we saw in the Chapter 2 the slow-roll parameters are defined as follows⁴⁶

$$\epsilon_V = \frac{M_{pl}^2}{2} \left(\frac{V'}{V}\right)^2 \quad \text{and} \quad \eta_V = M^2 \left(\frac{V''}{V}\right). \quad (3.4)$$

Replacing (3.4) in the scalar and tensor spectral indices and their corresponding running terms, i.e., (2.72), (2.73), (2.74), (2.75) and (2.76), we get the scalar and tensor spectral indices and their corresponding running terms in terms of the Starobinsky potential and their derivatives. The next step is replacing the inflation field in terms of N (3.3) in the Starobinsky potential and its derivatives, obtaining the following expressions for the slow-roll parameters:

$$\epsilon_V = \frac{3}{4 \left(1 - \frac{3}{4N}\right)^2 N^2}, \quad (3.5)$$

$$\eta_V = -\frac{8(-3 + 2N)}{(3 - 4N)^2}, \quad (3.6)$$

also,

$$\xi_V^2 \simeq \frac{64(-3 + N)}{(-3 + 4N)^3} \quad \text{and} \quad \varpi_V^3 \simeq -\frac{256(-6 + N)}{(3 - 4N)^4}. \quad (3.7)$$

Parameter	Symbol	Starobinsky	Planck
Tensor spectral index	n_t	-0.00042 ± 0.906	-0.0045 ± 0.0067
Scalar spectral index	n_s	0.9653 ± 0.0004	0.9649 ± 0.0042
Running of tensor spectral index	$\frac{dn_t}{d \ln k}$	-0.000014 ± 0.012	-
Running of scalar spectral index	$\frac{dn_s}{d \ln k}$	-0.00060 ± 0.53	-0.0013 ± 0.012
Running of running of scalar spectral index	$\frac{d^2 n_s}{d \ln k^2}$	-0.00002 ± 0.99	0.022 ± 0.012
Tensor-to-scalar ratio	r	<0.005	<0.11

Table 3.3: Values of scalar and tensor spectral indices, their corresponding running indices and tensor-to-scalar ratio, obtained from the Starobinsky model in a slow-roll approximation and reported by Planck satellite^{1,2}.

The scalar and tensor spectral indices and their respective running expressions computed in terms of N , are:

$$n_t \simeq -\frac{3}{2\left(1 - \frac{3}{4N}\right)^2 N^2}, \quad (3.8)$$

$$n_s \simeq \frac{(-15 + 4N)(1 + 4N)}{(3 - 4N)^2}, \quad (3.9)$$

$$\frac{dn_t(k)}{d \ln k} \simeq -\frac{768N}{(3 - 4N)^4}, \quad (3.10)$$

$$\frac{dn_s(k)}{d \ln k} \simeq -\frac{128N(9 + 4N)}{(3 - 4N)^4}, \quad (3.11)$$

$$\frac{d^2 n_s(k)}{d \ln k^2} \simeq -\frac{512N(27 + 4N(33 + 8N))}{(3 + 4N)^6}, \quad (3.12)$$

where the Planck mass has a value of 1 ($M = 1$). The tensor to-scalar ratio r in terms of N is giving by

$$r \simeq \frac{12}{\left(1 - \frac{3}{4N}\right)^2 N^2}. \quad (3.13)$$

The e -folding number that we use was 60 ($N = 60$), since is the value that favors the inflation epoch in the early Universe. The values that we obtain for the scalar and tensor spectral indices, their corresponding running terms and the tensor-to-scalar ratio are obtained Table 3.3.

Finally, the values presented in Table 3.3 are placed in the CAMB code, specifically in the **params.ini** file. From lines 84 to 88 of **params.ini** file were modified adding the values that we obtained.

```
#Initial power spectrum , amplitude , spectral index and running. Pivot k in
Mpc^{-1}.
initial_power_num          = 1
pivot_scalar               = 0.05
pivot_tensor               = 0.05
```

```
scalar_amp(1)           = 2.1e-9
scalar_spectral_index(1) = 0.96539
scalar_nrun(1)          = -0.000606132
scalar_nrunrun(1)       = -0.0000213479
tensor_spectral_index(1) = -0.000427282
tensor_nrun(1)          = -0.0000146056
```

After run the code the TT power spectrum data was obtained in a **test_scalCls.DAT** file and was plotted.

Chapter 4

Conclusions & Outlook

In this work, we reproduce the CMB temperature power spectrum with the Starobinsky inflationary model into the slow-roll approximation Figure 3.1. The TT power spectrum was divided in three parts: (a) “Sachs-Wolfe plateau” region ($\ell < 90$), (b) the acoustic peak region ($90 < \ell < 900$) and (c) The Silk damping region ($\ell > 900$). Each part was described and interpreted independently.

From the accurate reproduction of the TT power spectrum and the relative small value of tensor-to-scalar ratio ($r < 0.005$) is observed that the Starobinsky model into the slow-roll approximation is able to describe the early universe and its evolution. As we saw in Chapter 3, the differences between the amplitude values obtained from our model and the values that Planck satellite reports, affects directly to the cosmic parameters: age of universe, mass density Ω_m , baryon density $\Omega_b h^2$, spectral index n_s and tensor-to-scalar ratio r . The differences in the cosmic parameters values are related with small changes in the physics that the TT power spectrum describes.

The “Sachs-Wolfe plateau” region shows the lower differences between the TT power spectrum that we obtained and that Planck reports, meaning that the Starobinsky model describes with high accuracy the primordial fluctuations in the CMB. Also, the Starobinsky model and Planck data reported favors the presence of a inflationary epoch in early Universe. The Acoustic Peak region shows bigger differences in the amplitude of the peaks that are presented in this region. This differences are related with the value of matter and baryon density obtained from our model ($\Omega_m \approx 0.3158 \pm 0.001$ and $\Omega_b h^2 \approx 0.0223 \pm 0.0004$). From this we interpret that there was an additional load of mass and an increment in the inertia in the photon-baryon fluid at recombination epoch also the limit temperature is smaller in this epoch. The peaks and troughs that we obtain and those that report Planck satellite are located at the same multipole moment, except for the first peak that in Starobinsky TT power spectrum are located at 221ℓ . From the theory this affects to the age of the universe, this is confirmed by the Starobinsky model giving a universe age of 13.798 ± 0.007 . The Silk Damping region in the TT power spectrum reproduced by the Starobinsky model shows a shift to smaller angular scales, that is attributed to a photon-baryon fluid more tightly coupled at recombination and the decrease in $\Omega_b h^2 \approx 0.0223 \pm 0.0004$. Finally, the higher value of the scalar index ($n_s \approx 0.9653 \pm 0.0004$) reduce

the whole amplitude of the reproduced TT power spectrum, since it comes from the overall slope of the CMB power spectrum.

For future work is proposed the fit of the peaks and troughs of Acoustic peak region and Silk damping region in order to obtain theoretical values of cosmic parameters for the Starobinsky inflationary model into the slow-roll approximation. The process present in this work to obtain the temperature power spectrum can be reproduced with other inflationary models to verify its reliability.

Bibliography

- [1] Aghanim, N.; Akrami, Y.; Arroja, F.; Ashdown, M.; Aumont, J.; Baccigalupi, C.; Ballardini, M.; Banday, A. J.; Barreiro, R.; Bartolo, N.; et al., Planck 2018 results-I. Overview and the cosmological legacy of Planck. *Astronomy & Astrophysics* **2020**, *641*, A1.
- [2] Akrami, Y.; Arroja, F.; Ashdown, M.; Aumont, J.; Baccigalupi, C.; Ballardini, M.; Banday, A.; Barreiro, R.; Bartolo, N.; Basak, S.; et al., Planck 2018 results: X. Constraints on inflation. **2020**,
- [3] Alpher, R. A.; Herman, R. Evolution of the Universe. *Nature* **1948**, *162*, 774–775.
- [4] Penzias, A. A.; Wilson, R. W. A measurement of excess antenna temperature at 4080 Mc/s. *The Astrophysical Journal* **1965**, *142*, 419–421.
- [5] Tanabashi, M.; Group, P. D.; et al., Big-Bang Cosmology. *Review of particle physics* **2018**, *98*, 030001.
- [6] Durrer, R. The cosmic microwave background: the history of its experimental investigation and its significance for cosmology. *Classical and Quantum Gravity* **2015**, *32*, 124007.
- [7] Conklin, E. Velocity of the Earth with respect to the Cosmic Background Radiation. *Nature* **1969**, *222*, 971–972.
- [8] Smale, A.; Switzer, E.; Greason, M. LAMBDA - Cosmic Background Explorer. 2008; <https://lambda.gsfc.nasa.gov/product/cobe/>.
- [9] Hinshaw, G.; Larson, D.; Komatsu, E.; Spergel, D. N.; Bennett, C.; Dunkley, J.; Nolte, M.; Halpern, M.; Hill, R.; Odegard, N.; et al., Nine-year Wilkinson Microwave Anisotropy Probe (WMAP) observations: cosmological parameter results. *The Astrophysical Journal Supplement Series* **2013**, *208*, 19.
- [10] Bond, J.; Efstathiou, G. The statistics of cosmic background radiation fluctuations. *Monthly Notices of the Royal Astronomical Society* **1987**, *226*, 655–687.
- [11] Sachs, R.; Wolfe, A. Perturbations of a cosmological model and angular variations of the microwave background. 1967.
- [12] Sugiyama, N. Introduction to temperature anisotropies of Cosmic Microwave Background radiation. *Progress of Theoretical and Experimental Physics* **2014**, *2014*, 06B101.

- [13] Lewis, A. GetDist: a Python package for analysing Monte Carlo samples. **2019**,
- [14] Liddle, A. R.; Lyth, D. H. *Cosmological inflation and large-scale structure*; Cambridge university press, 2000.
- [15] Vázquez, J. A.; Padilla, L. E.; Matos, T. Inflationary cosmology: from theory to observations. *arXiv preprint arXiv:1810.09934* **2018**,
- [16] Ryden, B. *Introduction to cosmology*; Cambridge University Press, 2017.
- [17] Tsujikawa, S. Introductory review of cosmic inflation. *arXiv preprint hep-ph/0304257* **2003**,
- [18] Bernardeau, F.; Grojean, C.; Dalibard, J. *Particle physics and cosmology: the fabric of spacetime: lecture notes of the Les Houches Summer School 2006*; Elsevier, 2007.
- [19] de Boer, J.; Hartong, J.; Obers, N.; Sybesma, W.; Vandoren, S. Perfect fluids. *SciPost Physics* **2018**, 5, 003.
- [20] Riess, A. G.; Macri, L. M.; Hoffmann, S. L.; Scolnic, D.; Casertano, S.; Filippenko, A. V.; Tucker, B. E.; Reid, M. J.; Jones, D. O.; Silverman, J. M.; et al., A 2.4% determination of the local value of the Hubble constant. *The Astrophysical Journal* **2016**, 826, 56.
- [21] Lake, K. The flatness problem and Λ . *Physical review letters* **2005**, 94, 201102.
- [22] Lakhali, B. S.; Guezmir, A. The Horizon Problem. 2019.
- [23] Linde, A. *Particle physics and inflationary cosmology*; CRC press, 1990; Vol. 5.
- [24] Sapkota, N.; Adhikari, B. A Review on Cosmic Inflation. *International Journal of Current Research and Academic Review* **2017**, 5.
- [25] Liddle, A. R. An introduction to cosmological inflation. *High energy physics and cosmology* **1998**, 260.
- [26] Guth, A. H. Inflationary universe: A possible solution to the horizon and flatness problems. *Physical Review D* **1981**, 23, 347.
- [27] Liddle, A. R.; Parsons, P.; Barrow, J. D. Formalizing the slow-roll approximation in inflation. *Physical Review D* **1994**, 50, 7222.
- [28] Remmen, G. N.; Carroll, S. M. How many e-folds should we expect from high-scale inflation? *Physical Review D* **2014**, 90, 063517.
- [29] Adam, R.; Ade, P. A.; Aghanim, N.; Akrami, Y.; Alves, M.; Argüeso, F.; Arnaud, M.; Arroja, F.; Ashdown, M.; Aumont, J.; et al., Planck 2015 results-I. Overview of products and scientific results. *Astronomy & Astrophysics* **2016**, 594, A1.
- [30] Bennett, C. L.; Larson, D.; Weiland, J. L.; Jarosik, N.; Hinshaw, G.; Odegard, N.; Smith, K.; Hill, R.; Gold, B.; Halpern, M.; et al., Nine-year Wilkinson Microwave Anisotropy Probe (WMAP) observations: final maps and results. *The Astrophysical Journal Supplement Series* **2013**, 208, 20.

- [31] Bonga, B.; Gupta, B. Phenomenological investigation of a quantum gravity extension of inflation with the Starobinsky potential. *Physical Review D* **2016**, *93*, 063513.
- [32] Starobinsky, A. A. A new type of isotropic cosmological models without singularity. *Physics Letters B* **1980**, *91*, 99–102.
- [33] Kehagias, A.; Moradinezhad Dizgah, A.; Riotto, A. Remarks on the Starobinsky model of inflation and its descendants. *Physical Review D* **2014**, *89*.
- [34] De Felice, A.; Tsujikawa, S. $f(R)$ Theories. *Living Reviews in Relativity* **2010**, *13*.
- [35] Mishra, S. S.; Sahni, V.; Toporensky, A. V. Initial conditions for inflation in an FRW universe. *Physical Review D* **2018**, *98*, 083538.
- [36] Casadio, R.; Giugno, A.; Giusti, A. Corpuscular slow-roll inflation. *Physical Review D* **2018**, *97*, 024041.
- [37] Aldabergenov, Y.; Ishikawa, R.; Ketov, S. V.; Kruglov, S. I. Beyond Starobinsky inflation. *Physical Review D* **2018**, *98*, 083511.
- [38] Tapia, T.; Mughal, M. Z.; Rojas, C. Semiclassical analysis of the Starobinsky inflationary model. *Physics of the Dark Universe* **2020**, *30*, 100650.
- [39] Liguori, M.; Hansen, F. K.; Komatsu, E.; Matarrese, S.; Riotto, A. Testing primordial non-Gaussianity in CMB anisotropies. *Physical Review D* **2006**, *73*, 043505.
- [40] Hu, W.; Dodelson, S. Cosmic microwave background anisotropies. *Annual Review of Astronomy and Astrophysics* **2002**, *40*, 171–216.
- [41] Bucher, M. Physics of the cosmic microwave background anisotropy. *International Journal of Modern Physics D* **2015**, *24*, 1530004.
- [42] Challinor, A. CMB anisotropy science: a review. *Proceedings of the International Astronomical Union* **2012**, *8*, 42–52.
- [43] Tojeiro, R. Understanding the Cosmic Microwave Background temperature power spectrum. *alm* **2006**, *2*, 6.
- [44] Hinshaw, G.; Nolte, M.; Bennett, C.; Bean, R.; Doré, O.; Greason, M.; Halpern, M.; Hill, R.; Jarosik, N.; Kogut, A.; et al., Three-year wilkinson microwave anisotropy probe (wmap*) observations: Temperature analysis. *The Astrophysical Journal Supplement Series* **2007**, *170*, 288.
- [45] Ade, P.; Aghanim, N.; Arnaud, M.; Arroja, F.; Ashdown, M.; Aumont, J.; Baccigalupi, C.; Ballardini, M.; Banday, A.; Barreiro, R.; et al., Planck 2015 results-XX. Constraints on inflation. *Astronomy & Astrophysics* **2016**, *594*, A20.
- [46] Zarei, M. On the running of the spectral index to all orders: a new model-dependent approach to constrain inflationary models. *Classical and Quantum Gravity* **2016**, *33*, 115008.

- [47] Aghanim, N.; Akrami, Y.; Arroja, F.; Ashdown, M.; Aumont, J.; Baccigalupi, C.; Ballardini, M.; Banday, A. J.; Barreiro, R. B.; et al., Planck2018 results. *Astronomy Astrophysics* **2020**, *641*, A1.
- [48] Page, L.; Nolta, M.; Barnes, C.; Bennett, C.; Halpern, M.; Hinshaw, G.; Jarosik, N.; Kogut, A.; Limon, M.; Meyer, S.; et al., First-year Wilkinson Microwave Anisotropy Probe (WMAP)* observations: interpretation of the TT and TE angular power spectrum peaks. *The Astrophysical Journal Supplement Series* **2003**, *148*, 233.
- [49] Smoot, G. F.; Bennett, C. L.; Kogut, A.; Wright, E.; Aymon, J.; Boggess, N.; Cheng, E.; De Amici, G.; Gulkis, S.; Hauser, M.; et al., Structure in the COBE differential microwave radiometer first-year maps. *The Astrophysical Journal* **1992**, *396*, L1–L5.
- [50] Souradeep, T.; Saha, R.; Jain, P. Angular power spectrum of CMB anisotropy from WMAP. *New Astronomy Reviews* **2006**, *50*, 854–860.
- [51] Mohanty, S. *Astroparticle Physics and Cosmology*; Springer, 2020; pp 91–138.
- [52] Casas, S. Power Spectrum and the Anisotropies of the CMB.
- [53] Hu, W.; Fukugita, M.; Zaldarriaga, M.; Tegmark, M. Cosmic microwave background observables and their cosmological implications. *The Astrophysical Journal* **2001**, *549*, 669.
- [54] Keisler, R.; Reichardt, C.; Aird, K.; Benson, B.; Bleem, L.; Carlstrom, J.; Chang, C.; Cho, H.; Crawford, T.; Crites, A.; et al., A measurement of the damping tail of the cosmic microwave background power spectrum with the South Pole Telescope. *The Astrophysical Journal* **2011**, *743*, 28.
- [55] Hu, W.; Sugiyama, N.; Silk, J. The physics of microwave background anisotropies. *Nature* **1997**, *386*, 37–43.
- [56] Pettini, M. FLUCTUATIONS IN THE COSMIC MICROWAVE BACKGROUND. 2021.